



**HAL**  
open science

## The abundance of the long intergenic non-coding RNA 01087 differentiates between luminal and triple-negative breast cancers and predicts patient outcome

Fatima Domenica Elisa de Palma, Valentina del Monaco, Jonathan Pol, Margerie Kremer, Valeria D'argenio, Gautier Stoll, Donatella Montanaro, Barbara Uszczyńska-Ratajczak, Cecilia C Klein, Anna Vlasova, et al.

### ► To cite this version:

Fatima Domenica Elisa de Palma, Valentina del Monaco, Jonathan Pol, Margerie Kremer, Valeria D'argenio, et al.. The abundance of the long intergenic non-coding RNA 01087 differentiates between luminal and triple-negative breast cancers and predicts patient outcome. *Pharmacological Research*, 2020, 161, pp.105249. 10.1016/j.phrs.2020.105249 . hal-03351350

**HAL Id: hal-03351350**

**<https://hal.sorbonne-universite.fr/hal-03351350v1>**

Submitted on 22 Sep 2021

**HAL** is a multi-disciplinary open access archive for the deposit and dissemination of scientific research documents, whether they are published or not. The documents may come from teaching and research institutions in France or abroad, or from public or private research centers.

L'archive ouverte pluridisciplinaire **HAL**, est destinée au dépôt et à la diffusion de documents scientifiques de niveau recherche, publiés ou non, émanant des établissements d'enseignement et de recherche français ou étrangers, des laboratoires publics ou privés.



Contents lists available at ScienceDirect

## Pharmacological Research

journal homepage: [www.elsevier.com/locate/yphrs](http://www.elsevier.com/locate/yphrs)

## The abundance of the long intergenic non-coding RNA 01087 differentiates between luminal and triple-negative breast cancers and predicts patient outcome

Fatima Domenica Elisa De Palma<sup>a,b,c,\*,1</sup>, Valentina Del Monaco<sup>a,1</sup>, Jonathan G. Pol<sup>b,c,1</sup>, Margerie Kremer<sup>b,c</sup>, Valeria D'Argenio<sup>a,d</sup>, Gautier Stoll<sup>b,c</sup>, Donatella Montanaro<sup>a</sup>, Barbara Uszczyńska-Ratajczak<sup>e,f</sup>, Cecilia C. Klein<sup>e,g,h</sup>, Anna Vlasova<sup>e</sup>, Gerardo Botti<sup>i</sup>, Massimiliano D'Aiuto<sup>i</sup>, Alfonso Baldi<sup>a,j</sup>, Roderic Guigó<sup>e,k</sup>, Guido Kroemer<sup>b,c,l,m,n</sup>, Maria Chiara Maiuri<sup>b,c,\*,2</sup>, Francesco Salvatore<sup>a,o,p,\*,2</sup>

<sup>a</sup> CEINGE-Biotecnologie Avanzate s.c.ar.l, Naples 80145, Italy

<sup>b</sup> Team "Metabolism, Cancer & Immunity", Centre de Recherche des Cordeliers, INSERM UMR1138, Sorbonne Université, Université de Paris, Paris 75006, France

<sup>c</sup> Metabolomics and Cell Biology Platforms, Gustave Roussy Cancer Campus, Villejuif 94805, France

<sup>d</sup> San Raffaele Open University, Rome 00166, Italy

<sup>e</sup> Bioinformatics and Genomics, Centre for Genomic Regulation (CRG), Barcelona 08003, Catalonia, Spain

<sup>f</sup> Institute of Bioorganic Chemistry, Polish Academy of Sciences, Poznan, Poland

<sup>g</sup> Departamento de Genética, Microbiología i Estadística, Facultat de Biologia and Institut de Biomedicina (IBUB), Universitat de Barcelona, Barcelona, Spain

<sup>h</sup> Clarivate Analytics, Barcelona, Spain

<sup>i</sup> Department of Senology, Istituto Nazionale Tumori - IRCCS Fondazione Pascale, Naples, Italy

<sup>j</sup> Department of Environmental, Biological and Pharmaceutical Sciences and Technologies, University of Campania "Luigi Vanvitelli", Caserta, 81100 Italy

<sup>k</sup> Universitat Pompeu Fabra (UPF), Barcelona, Spain

<sup>l</sup> Pôle de Biologie, Hôpital Européen Georges Pompidou, Assistance Publique-Hôpitaux de Paris, Paris, France

<sup>m</sup> Suzhou Institute for Systems Medicine, Chinese Academy of Medical Sciences, Suzhou, China

<sup>n</sup> Department of Women's and Children's Health, Karolinska Institute, Karolinska University Hospital, Stockholm, Sweden

<sup>o</sup> Department of Molecular Medicine and Medical Biotechnologies, University of Naples Federico II, Naples 80131, Italy

<sup>p</sup> Inter-University Center for multifactorial and multi genetic chronic human diseases, "Federico II" - Naples, Tor Vergata- Roma II, and Chieti-Pescara Universities, Italy

## ARTICLE INFO

## Keywords:

LINC01087  
Long non-coding RNA  
Breast cancer  
Luminal breast cancer  
Triple-negative breast cancer  
Biomarker

## ABSTRACT

The molecular complexity of human breast cancer (BC) renders the clinical management of the disease challenging. Long non-coding RNAs (lncRNAs) are promising biomarkers for BC patient stratification, early detection, and disease monitoring. Here, we identified the involvement of the long intergenic non-coding RNA 01087 (LINC01087) in breast oncogenesis. LINC01087 appeared significantly downregulated in triple-negative BCs (TNBCs) and upregulated in the luminal BC subtypes in comparison to mammary samples from cancer-free women and matched normal cancer pairs. Interestingly, deregulation of LINC01087 allowed to accurately distinguish between luminal and TNBC specimens, independently of the clinicopathological parameters, and of the histological and *TP53* or *BRCA1/2* mutational status. Moreover, increased expression of LINC01087 predicted a better prognosis in luminal BCs, while TNBC tumors that harbored lower levels of LINC01087 were associated with reduced relapse-free survival. Furthermore, bioinformatics analyses were performed on TNBC and luminal BC samples and suggested that the putative tumor suppressor activity of LINC01087 may rely on interferences with pathways involved in cell survival, proliferation, adhesion, invasion, inflammation and drug

\* Corresponding authors at: CEINGE-Biotecnologie Avanzate s.c.ar.l, Naples 80145, Italy.

E-mail addresses: [depalma@ceinge.unina.it](mailto:depalma@ceinge.unina.it) (F.D.E. De Palma), [validelmonaco@gmail.com](mailto:validelmonaco@gmail.com) (V. Del Monaco), [pol\\_jonathan@yahoo.fr](mailto:pol_jonathan@yahoo.fr) (J.G. Pol), [margerie.kremer@orange.fr](mailto:margerie.kremer@orange.fr) (M. Kremer), [dargenio@ceinge.unina.it](mailto:dargenio@ceinge.unina.it) (V. D'Argenio), [gautier.stoll@upmc.fr](mailto:gautier.stoll@upmc.fr) (G. Stoll), [montanaro@ceinge.unina.it](mailto:montanaro@ceinge.unina.it) (D. Montanaro), [barbara.uszczyńska@gmail.com](mailto:barbara.uszczyńska@gmail.com) (B. Uszczyńska-Ratajczak), [ceciklein@gmail.com](mailto:ceciklein@gmail.com) (C.C. Klein), [vlasova.av@gmail.com](mailto:vlasova.av@gmail.com) (A. Vlasova), [g.botti@istitutotumori.na.it](mailto:g.botti@istitutotumori.na.it) (G. Botti), [massimiliano.daiuto@gmail.com](mailto:massimiliano.daiuto@gmail.com) (M. D'Aiuto), [alfonsobaldi@tiscali.it](mailto:alfonsobaldi@tiscali.it) (A. Baldi), [roderic.guigo@crg.cat](mailto:roderic.guigo@crg.cat) (R. Guigó), [kroemer@orange.fr](mailto:kroemer@orange.fr) (G. Kroemer), [chiara.maiuri@upmc.fr](mailto:chiara.maiuri@upmc.fr) (M.C. Maiuri), [salvator@unina.it](mailto:salvator@unina.it) (F. Salvatore).

<sup>1</sup> equal contributors.

<sup>2</sup> co-last authors.

<https://doi.org/10.1016/j.phrs.2020.105249>

Received 21 September 2020; Received in revised form 8 October 2020; Accepted 8 October 2020

Available online 14 October 2020

1043-6618/© 2020 The Authors.

Published by Elsevier Ltd.

This is an open access article under the CC BY-NC-ND license

(<http://creativecommons.org/licenses/by-nc-nd/4.0/>).

sensitivity. Altogether, these data suggest that the assessment of LINC01087 deregulation could represent a novel, specific and promising biomarker not only for the diagnosis and prognosis of luminal BC subtypes and TNBCs, but also as a predictive biomarker of pharmacological interventions.

## 1. Introduction

Breast cancer (BC) is a heterogeneous group of diseases distinguishable by their biological and clinical features [1]. Based on the immunohistochemical expression of the progesterone receptor (PR), estrogen receptor (ER), Erb-B2 receptor tyrosine kinase 2 (ERBB2, best known as the human epidermal growth factor receptor 2, HER2) and the proliferation marker Ki67, BCs have been classified into four surrogate intrinsic subtypes: luminal A (lumA), luminal B (lumB), HER2 positive (HER2<sup>+</sup>) and triple-negative breast cancer (TNBC) [1,2].

Among BC subtypes, TNBC regroups tumors with different clinical, histological and molecular imprints [1]. TNBC is clinically defined by a lack of ER, PR and HER2 receptors and does not respond to the precision medicines currently approved for the care of the other types of BC, such as the immunotherapies with pertuzumab and trastuzumab, or targeted chemotherapy with lapatinib [3]. However, a phase III trial showed an enhancement of the anticancer activity of the immunotherapy atezolizumab when combined with nanoparticle albumin-bound (nab)-paclitaxel on the progression-free survival (PFS) of metastatic TNBC patients [4]. Moreover, polyadenosine diphosphate-ribose polymerase (PARP) inhibitors (i.e. olaparib) have been used in metastatic TNBC patients that harbor mutation in *BRCA1* gene [5]. TNBCs are particularly aggressive, exhibiting a high risk of recurrence and metastasis, as well as the worst prognosis compared to the other BC subsets [3,6].

Luminal BCs are clinically defined as hormone-receptor positive tumors: ER<sup>+</sup> and/or PR<sup>+</sup> [1]. Additionally, lumA BCs are HER2- Ki67<sup>low</sup> whereas lumB BCs can be either HER2<sup>+</sup> or HER2- Ki67<sup>high</sup>. In comparison to TNBCs, the luminal subtypes are associated with better prognosis and survival, lumB having a slightly worse prognosis than lumA BCs [1]. The management of luminal BC subtypes depend on various criteria including prognostic and predictive factors as well as comorbidities. Generally, lumA and HER2- lumB BCs at early stages are treated by endocrine therapy and can be implemented with chemotherapy (i.e. anthracycline and/or taxanes), especially for patients at high risk of recurrence [1,3]. In patients with advanced tumors and that do not present visceral crisis or significant organ function impairment, endocrine therapy alone or in combination with drugs (i.e. cyclin-dependent kinases (CDK) 4/6 inhibitors or everolimus) represents the first line of treatment [1,3,7,8]. Concerning HER2<sup>+</sup> lumB patients, early BCs with tumor size over 1 centimeter or with axillary lymph node involvement usually benefit from chemotherapy plus a dual HER2-targeted therapy (trastuzumab and pertuzumab) and in association with adjuvant hormone therapy. Instead, advanced HER2<sup>+</sup> lumB BCs are treated with anti-HER2 agents plus chemotherapy [1,3].

Advancements in the ‘omics’ technologies have provided a deeper understanding of the molecular heterogeneity within and between BC subtypes, identifying promising genetic and epigenetic biomarkers [9]. In fact, BC molecular signatures, in association with the canonical histological tests, not only improved disease detection but also its therapeutic management [9,10].

An increasing number of studies is exploring the role of long non-coding RNAs (lncRNAs) in human diseases, such as BC [11–13]. lncRNAs consist of mRNA-like molecules longer than 200 nucleotides in length that have no or limited protein-coding potential [14,15]. They are involved in a variety of cellular phenomena such as epigenetic, transcriptional and post-transcriptional regulation as well as chromatin remodeling [16]. However, the majority of lncRNAs remains functionally uncharacterized [17]. lncRNAs can be classified into five main categories: sense, antisense, bidirectional, intronic and intergenic, according to their position and direction of synthesis on the genome with

respect to the nearest protein coding gene [18]. The involvement of lncRNAs in breast carcinogenesis, metastasis and chemotherapy resistance has been reported [13,19–21]. In addition, due to their dysregulated expression, some lncRNAs have been recognized as promising subtype-specific biomarkers for early detection of BC and disease monitoring [19,22].

In the present study, we investigated the clinical role of the long intergenic non-coding RNA 01087 (LINC01087) in BC tissues. We assessed: i) LINC01087 expression in different molecular and histological human BC subtypes; ii) its association with the mutational status of *TP53* and *BRCA1/2*; iii) the prognostic value of LINC01087 in TNBC, lumA and lumB BCs; and iv) LINC01087 cellular network through in-depth bioinformatic analyses.

Our findings indicate that aberrant expression of LINC01087 may contribute to breast oncogenesis. LINC01087 could be considered as a novel and highly specific diagnostic marker of luminal and TNBC molecular subtypes. Precisely, in comparison to healthy breast tissue, the downregulation of LINC01087 was associated with TNBCs whereas its upregulation was characteristic of the luminal subtypes. Moreover, LINC01087 demonstrated a prognostic interest, with a lower level of LINC01087 indicating a worse prognosis in TNBC patients but a better prognosis in luminal patients.

## 2. Materials and Methods

### 2.1. Patient samples

Sixty-one breast tissue specimens (17 luminal A, 9 luminal B, 4 HER2<sup>+</sup> and 15 TNBC breast tumor samples, 12 paired adjacent non-tumor tissues, 4 normal tissues derived from plastic surgery) were collected from cancer patients attending the Senology Department of the “Istituto Nazionale dei Tumori - Fondazione G. Pascale” of Naples, Italy. All breast tissues were snap-frozen in liquid nitrogen after surgery and cryopreserved at -80° before their analysis. Histological and molecular tests were performed to evaluate the immunoprofile of each breast tissue. All patients provided their written informed consent for the research purpose of these clinical materials according to the tenets of the Helsinki Declaration. This study was approved by the Istituto Nazionale Tumori - Fondazione G. Pascale Ethics Committee (protocol number 3 of 03/25/2009).

### 2.2. Laser-capture microdissection

Human breast tissue samples were all subjected to laser-capture microdissection (LCM). Frozen sections of each tissue sample were embedded in Optimal Cutting Temperature (OCT) compound, cut at 14 μm thickness and placed on polyethylene sulfide (PPS) membrane slides (Microdissect GmbH, Herborn, Germany). Then, all PPS slides were fixed in 70% ethanol for 1 minute, stained with haematoxylin and eosin for 30 seconds, followed by three dehydration steps in 90%, 95% and 99% ethanol for 1 minute each, then air-dried. Finally, about 10 to 20 million μm<sup>2</sup> of microdissected tissue were obtained from each stained sample using Leica LMD6000 microdissection system (Wetzlar, Germany), according to the manufacturer’s instructions.

### 2.3. RNA extraction and reverse transcription-quantitative real-time PCR

Total RNAs were extracted from microdissected tissues or cells in culture using Qiazol Lysis reagent and purified with RNeasy Mini Kit (Qiagen, Hilden, Germany). RNA quantity and purity were evaluated by

NanoDrop2000 (Thermo Fisher Scientific, Waltham, MA, USA), whereas RNA integrity (RIN) was assessed using the Experion™ Automated Electrophoresis System (Bio-Rad Laboratories, Hercules, CA, USA).

LINC01087 RNA expression was evaluated by reverse transcription-quantitative real-time PCR (RT-qPCR). First, 1 µg of total RNA was reverse transcribed using Superscript IV VILO Master MIX (Thermo Fisher Scientific). Then, 100 ng of cDNA were amplified with specific LINC01087 Taqman probe (Hs01902268\_u1, Thermo Fisher Scientific), carrying out the qPCR on the StepOne Real-time PCR system (Applied Biosystems, Foster City, CA, USA), according to the manufacturer's instructions. Relative gene expression was calculated according to the  $2^{-\Delta\Delta Ct}$  method, normalizing the level of LINC01087 to GAPDH mRNA, the endogenous control. Samples were run in three replicates per experiment. Data were represented as mean  $\pm$  standard deviation (SD) and were analyzed using GraphPad Prism software package (Graphpad® Software, San Diego, CA, USA). P-value  $\leq 0.05$  was considered statistically significant.

#### 2.4. High-throughput RNA sequencing

Ribo-Zero Gold rRNA removal kit was used to remove ribosomal RNA from 500 ng of total RNA according to the manufacturer's recommendations. Next, total purified RNA was used to generate cDNA indexed libraries by using the TruSeq® Stranded Total RNA Sample Preparation kit. Briefly, double-stranded cDNA fragments were synthesized from total purified RNAs, ligated to adaptors after being end-repaired and adenylated, then enriched by PCR amplification. After, PCR products were purified using AMPure XP beads (Beckman Coulter, Brea, CA, USA), quantified and quality assessed on the Agilent Bioanalyzer 2100 system (Agilent Technologies). Finally, indexed libraries were pooled in equimolar ratios before sequencing. Sequencing was carried out on the Illumina HiSeq 1500 platform to generate 100 bp paired-end reads, following the manufacturer's protocols. All reagents (unless specified otherwise) were purchased from Illumina Inc (San Diego, CA, USA).

#### 2.5. Cell culture

Human breast cancer cell lines (MCF7, BT474, BT549, HCC1937, BT20, Hs578 T) and one normal human breast cell line (MCF10A) were kindly provided by the cell culture facility of CEINGE-Biotecnologie Avanzate s.c.a.r.l. (Naples, Italy). MCF10A cells were maintained in Dulbecco's modified Eagle medium/nutrient mixture F-12 (DMEM/F12) supplemented with epidermal growth factor (EGF) 20 ng/ml, insulin 10 µg/ml, hydrocortisone 0.5 mg/ml, cholera toxin 100 ng/ml, 5% equine serum and 1% penicillin–streptomycin. MCF7 cells were cultured in Eagle's minimum essential medium (EMEM) supplemented with 2 mM glutamine, 1% non-essential amino acids (NEAA), 10% fetal bovine serum (FBS) and 1% penicillin–streptomycin. All the other breast cancer cell lines were maintained in Roswell Park Memorial Institute (RPMI)-1640 medium, supplemented with 10% of FBS and 1% penicillin–streptomycin. Cells were cultured in a humidified atmosphere containing 5% CO<sub>2</sub> at 37 °C. All cell lines were negative for mycoplasma contamination and were passaged  $<10$  times after and reviving the frozen stocks. All reagents (unless specified otherwise) were purchased from Sigma-Aldrich (St. Louis, MO, USA). The media and supplements for cell culture were purchased from Gibco-Life Technologies™ (Grand Island, NY, USA) and plasticware from Corning Inc (New York, NY, USA).

### 3. Bioinformatics and statistical analyses

#### 3.1. Transcriptomic data analysis

RNA-seq data were processed using grape-nf pipeline (<https://github.com/guigolab/grape-nf>). Reads were aligned to the human reference

genome hg19 with STAR 2.4.0 j [23]. GENCODE reference annotation (v19) was used to guide the aligner [15]. Up to 4 mismatches per alignment were allowed. In particular, we used: “–out-FilterMismatchNoverReadLmax 0.04” parameter that is listed as one of the ENCODE standard options that are specified in the STAR manual [24]. Gene and transcript quantifications were performed using RSEM [25]. Differentially expressed lncRNAs were identified using limma R/Bioconductor package (v3.5.0). Resulting empirical Bayes moderated t p-values were adjusted by Benjamini-Hochberg (BH) procedure. Only lncRNAs with an associated adjusted p-value  $\leq 0.05$  and absolute log<sub>2</sub> Fold Change  $\geq 2$  were considered to be differentially expressed.

For *in silico* analyses, RNA-seq data of BC patients from the Cancer Genome Atlas (TCGA) were downloaded from the website Genomic Data Commons (<https://portal.gdc.cancer.gov>), and data on breast cell lines from the Expression Atlas database (<http://www.ebi.ac.uk/gxa>) (Supplementary Table S16). Analysis of lncRNA differential expression was performed using limma R/Bioconductor. Resulting empirical Bayes moderated t p-values were adjusted using the Benjamini-Hochberg (BH) procedure. A gene was determined as significantly differentially expressed when the adjusted p-value was  $\leq 0.05$  and absolute log<sub>2</sub> FC was  $\geq 2$ . The edgeR R/Bioconductor package was applied to normalize RNA-seq data with consideration for lncRNAs only.

Receiver operating characteristic (ROC) curves were generated and area under the ROC curves (AUC) was calculated to assess the diagnostic value of LINC01087 using “caret”, “MASS”, “verification” and “pROC” R packages [26,27].

Fisher's exact and Wilcoxon rank-sum tests were executed to compare the expression of LINC01087 between i) BC subtypes; ii) clinicopathological parameters; iii) histological status and iv) BRCA1, BRCA2 and TP53 mutational status in BC patients (cBioPortal data, <http://www.cbioportal.org>) (Supplementary Table S16).

#### 3.2. Survival curve analysis

To test the role of LINC01087 as a biomarker of BC prognosis, survival curves were plotted using an online survival analysis tool, namely “Kaplan-Meier Plotter” (<http://kmplot.com/analysis/>). The effect of the down-expression of LINC01087 was explored on RFS, DMFS and OS by merging data from different datasets. The individual datasets used are listed in Supplementary Table S3. Survival curves were generated by selecting as filters “the best cutoff” and “JetSet best probe set”. Forest plots were generated with meta R package using the results computed with the Kaplan-Meier Plotter on the basis of pan-cancer sequencing data (Supplementary Table S16).

#### 3.3. GO, KEGG, REACTOME and STRING analyses

Segregation between TNBC patients of the TCGA database with intermediate (TNBC LINC01087<sup>int</sup>) versus low (TNBC LINC01087<sup>lo</sup>) expression levels of LINC01087 was established using a cut-off value of 0.0242 CPM. Segregation between luminal BCs with high (lum LINC01087<sup>hi</sup>) versus intermediate (lum LINC01087<sup>int</sup>) levels of LINC01087 was established using a cut-off value of 3.331 CPM. Computed cut-off values matched LINC01087 expression in normal samples, with LINC01087<sup>lo</sup> corresponding to the first quartile and LINC01087<sup>hi</sup> to the fourth (Fig. 1c). Limma R/Bioconductor package determining the coding genes that were differentially expressed in TNBC and luminal BCs. GO terms annotation was performed using the Ensembl BioMart tool ([www.ensembl.org](http://www.ensembl.org)), and KEGG and REACTOME pathways annotation was performed by means of the Comparative Toxicogenomics Database (ctdbase.org) (Supplementary Table S16). We used the R package gprofiler2 for GO, KEGG and REACTOME pathway enrichment analyses (p-value were adjusted using the Benjamini-Hochberg procedure). Protein-protein interaction (PPI) network was computed using the application programming interface (API) of the STRING database (string-db.org) in order to draw an interaction network representing

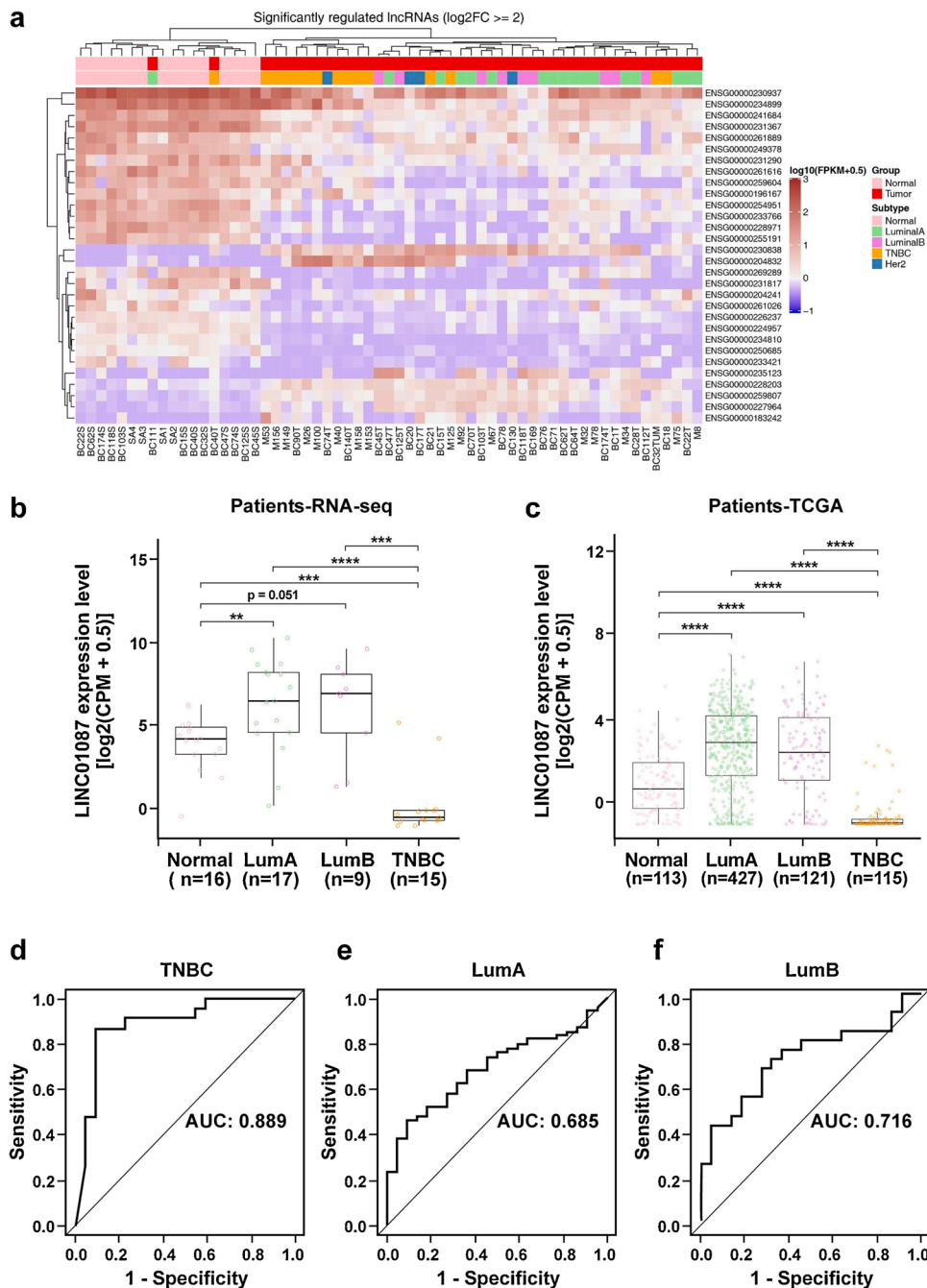


**Fig. 1.** LINC01087 is deregulated across normal and tumor breast samples. (a) Heatmap demonstrating differential expression of lncRNAs between normal breast tissues and overall breast tumors. Each column represents a breast tissue sample whose attributed molecular subtype is color-coded in the top bar of the heatmap. Each row represents a single lncRNA identified by its corresponding Ensembl ID. Individual values are expressed as  $\log_{10}(FPKM + 0.5)$ . (b, c) Box plots illustrating the level of expression of LINC01087 in normal and malignant human breast samples derived from (b) the RNA-seq data set and (c) the TCGA database. Box and whisker plots illustrate the expression level of LINC01087 as  $\log_2(CPM + 0.5)$ . Data show median, quartiles, and individual values. Data were compared using Wilcoxon rank-sum test,  $**p \leq 0.01$ ,  $***p \leq 0.001$ ,  $****p \leq 0.0001$ . (d-f) Diagnostic value of LINC01087 in BC. ROC curve analysis of LINC01087 in TNBC (d), luminal A (e) and luminal B (f) tissues. LINC01087 expression levels were extracted from the TCGA database. AUC, area under the curve; CPM, count per million; FC, fold change; FPKM, fragments per kilobase of exon per million fragments mapped; HER2, epidermal growth factor receptor 2; Lum A, luminal A; Lum B, luminal B; ROC, receiver operating characteristic; TNBC, triple-negative breast cancer.

only "experimentally determined" direct interactions. As an input, we selected the genes that were associated with GO terms represented by  $\geq 20$  genes for luminal A BC and TNBC, and by  $\geq 5$  genes for luminal B BC. In particular, we used the API to obtain a file containing the most confident interactions of each protein (i.e. with the highest combined scores, corresponding to the column "score" in the output file) [28]. Then, the "neighbor" proteins corresponding to interactions with an "experimentally determined" score ("escore")  $>0$  were selected. Two and five interactants were displayed in the network for each selected protein in the lumA and lumB analyses, respectively. Finally, the network with the selected proteins was graphed using the STRING database. In this representation, each protein corresponds to a node and the experimentally validated interactions between proteins are represented by edges.

#### 4. Results

##### 4.1. lncRNA expression profile in human breast samples

To identify a lncRNA signature in BC subtypes and to examine the role of a dysregulated expression of lncRNAs in breast carcinogenesis, we applied two complementary approaches.

First, we investigated the expression profile of lncRNAs by high-throughput sequencing of rRNA-depleted RNA samples extracted from 61 laser-microdissected breast tissues (Fig. 1a).

A total of 30 lncRNAs appeared differentially expressed (DE) between normal and malignant breast samples using a  $p\text{-value} \leq 0.05$  and an absolute  $\log_2FC \geq |2|$  as filters (Fig. 1a). For the subsequent analysis, we evaluated the expression profile of lncRNAs across different BC subtypes. Forty-four and 43 lncRNAs displayed differential expression

between TNBC and normal breast, or lumA BC, respectively (**Supplementary Figure S1a, b; Supplementary Table S1**).

Next, in order to extend the cohort of samples and to validate the DE lncRNAs identified in the transcriptomic analysis, available TCGA data from 813 samples (113 normal, 427 lumA, 121 lumB, 37 HER2<sup>+</sup> and 115 TNBC patients) were screened for differential expression of lncRNAs *in silico*. Among the 9789 lncRNAs detected, 14 long intergenic non-coding RNAs (LINC) were identified as DE across BC classes, using a  $p\text{-value} \leq 0.05$  and a  $\log_2FC \geq |0.585|$  as filters (**Supplementary Figure S1c, Supplementary Table S2**).

#### 4.2. LINC01087 expression is deregulated in TNBC and in luminal BC tissues

Among the list of lncRNAs significantly modulated in our RNA-sequencing (RNA-Seq) dataset of BC patients, LINC01087 exhibited a decreased expression specifically in TNBC versus normal breast tissues ( $\log_2FC = -2.5$ ,  $p = 0.016$ ; **Fig. 1b, Supplementary Figure S1, Supplementary Table S1**). This sharp drop in the expression of LINC01087 in TNBC was not only confirmed by RT-qPCR on the same samples (**Supplementary Figure S2a**), but also by interrogating the TCGA database (**Fig. 1c, Supplementary Figure S1c, Supplementary Table S2**).

Additionally, our transcriptomic analysis revealed an increased expression of LINC01087 specifically in both lumA and lumB BCs as compared to normal breast tissues (**Fig. 1b, Supplementary Figure S1, Supplementary Table S1**). Despite being insignificant by RT-qPCR (**Supplementary Figure S2a**), this enhanced level of LINC01087 in luminal BCs versus normal samples was validated in the cohorts recorded in the TCGA databank (**Fig. 1c, Supplementary Figure S1c, Supplementary Table S2**).

Importantly, LINC01087 exhibited the largest delta of expression out of the 43 lncRNAs differentially regulated between TNBC and lumA BC samples:  $\log_2FC = -5.8$ ,  $p = 0.0002$  (**Supplementary Table S1**). The same observation was made across the 26 lncRNAs that showed differential levels of expression between TNBC and lumB BC tissues:  $\log_2FC = -5.6$ ,  $p = 0.0009$  (**Supplementary Table S1**).

To confirm the diagnostic performance of LINC01087 in TNBC and luminal BCs, receiver operating characteristic (ROC) curves were built using TCGA data. The computed area under the ROC curves (AUC) indicated that the level of LINC01087 is a good diagnostic biomarker of TNBC (AUC = 0.889;  $p = 3.91e-06$ ), and a fair biomarker of luminal BCs (lumA: AUC = 0.685;  $p = 0.0037$ ; lumB: AUC = 0.716;  $p = 0.0058$ ) (**Fig. 1d-f**).

Regarding the expression level of LINC01087 in HER2<sup>+</sup> samples, it also appeared downregulated in the TCGA analysis compared to normal and luminal breast tissues (**Supplementary Figure S2b**). Nevertheless, due to a limited number of HER2<sup>+</sup> samples in our cohort ( $n = 4$ ) (**Supplementary Figure S2c**) and the conflicting results with respect to the TCGA data ( $n = 37$ ) (**Supplementary Figure S2b**), interpretation of the RNA-sequencing data did not allow to conclude on the expression levels of LINC01087 in HER2<sup>+</sup> samples.

The altered expression of LINC01087 was also witnessed in BC cell lines, first *in silico* by extracting its expression values from the Expression Atlas database, then *in vitro* by quantitating it in human breast cell lines (**Supplementary Figure S2d, e**).

Altogether, these data revealed that LINC01087 was significantly downregulated in TNBCs and upregulated in luminal BCs and that assessing its level could distinguish/diagnose these BC subtypes.

#### 4.3. LINC01087 deregulation predicts the clinical outcome of TNBC and luminal BC patients

To analyze the prognostic value of LINC01087, we investigated the association between LINC01087 expression and overall survival (OS) and relapse-free survival (RFS) in patients affected with various types of cancers, through Kaplan-Meier Plotter (KMplot) web-based tool

(kmplot.com) on the basis of pan-cancer sequencing data [29]. The forest plot illustrated that LINC01087 expression was predictive of a significant extension of OS in no less than 6 cancer types, among which BC ranked third (HR = 0.63, 95% CI = 0.46-0.87,  $p = 5e-03$ ), after thyroid and liver carcinomas (**Fig. 2**). Moreover, expression of LINC01087 was associated with a longer RFS in BC, which ranked first among different types of cancer (HR = 0.54, 95% CI = 0.35-0.83,  $p = 5e-03$ ) (**Supplementary Figure S3**).

Additionally, we used publicly available data of BC patients from the KMplot database. KMplot allowed to assess the impact of LINC01087 on the survival of multiple cohorts extracted from various databases, such as Gene Expression Omnibus (GEO). The effect of the down-expression of LINC01087 was explored particularly on RFS and, when the number of samples available in the database was sufficient, on distant metastasis-free survival (DMFS) and OS, by merging data from different datasets (**Fig. 3**). A summary of the individual datasets used for the estimation of each survival curve is given in **Supplementary Table S3**.

In a first analysis comprising BC tissues without further consideration of their subtype classification, patients presenting a reduced expression of LINC01087 in BC samples exhibited lower RFS ( $n = 1764$ ;  $p < 1e-16$ ), DMSF ( $n = 664$ ;  $p = 0.0007$ ) and OS ( $n = 626$ ;  $p = 7.3e-06$ ) (**Fig. 3a-c**). Overall, low expression of LINC01087 correlated with poorer clinical outcome.

High-throughput techniques permitted to refine patient prognosis and response to treatments based not only on immunohistochemical markers (ER, PR and HER2) and the traditional clinicopathological variables (tumor size, tumor grade and nodal involvement), but also on gene expression patterns. KMplot allows filtering BC patients according to the receptor and lymph node status, histological grade, type of treatment as well as tumor intrinsic subtype. The latter is defined based on immunohistochemical markers (ER, PR and HER2) and can be further sub-classified according to gene expression patterns.

In this line, we restricted LINC01087-related RFS analyses to TNBC cases, defined as ER-, PR- and HER2- BC patients (**Fig. 3d**). In addition, we analyzed LINC01087-related RFS in TNBC patients of the basal-like breast cancer (BLBC) subtype (**Fig. 3e**). The BLBC subtype is defined by a cluster of genes expressed in the basal or outer layer of the mammary gland epithelium. It accounts for about 60-90% of TNBCs and is characterized by an aggressive clinical course and resistance to targeted therapies [30]. Low expression of LINC01087 correlated with poorer RFS in TNBC patients ( $n = 161$ ;  $p = 2e-04$ ), including the most prevalent subtype, BLBC ( $n = 118$ ;  $p = 0.00012$ ) (**Fig. 3d, e**).

Current routine clinical management of breast cancer is also based on the evaluation of the histological tumor grade and nodal involvement. These two parameters are widely recognized as markers of aggressiveness and are related to a poorer prognosis in BC patients [1, 31]. Thus, to strengthen the prognostic role of a down-expression of LINC01087 in TNBCs, we evaluated the RFS of patients diagnosed with advanced TNBC (i.e. positive lymph node status [N<sup>+</sup>] and grade 3 [G3] tumor) harboring or not basal-like features (**Fig. 3f,g**). In these aggressive TNBCs, the expression level of LINC01087 was remarkably predicting patient outcome, independently of the BLBC sub-classification. Indeed, worsen RFS was observed in TNBC patients whose aggressive tumor expressed low levels of LINC01087 ( $n = 29$ ;  $p = 7e-04$ ), particularly the most prevalent subtype: BLBC ( $n = 22$ ;  $p = 1e-04$ ) (**Fig. 3f, g**). These multivariate analyses evidenced an association between a low expression of LINC01087 and a worsen outcome in all selected cohorts, particularly of the TNBC subtype.

Similarly to TNBC, the relationship between LINC01087 upregulation and the survival of luminal patients has been explored using KMplot. In particular, we used different datasets to evaluate the effect of the overexpression of LINC01087 on RFS and OS (**Fig. 3h-j**). The individual datasets used for the estimation of each survival curve are listed in **Supplementary Table S3**.

High expression of LINC01087 correlated with extended RFS in patients affected with lumA ( $n = 841$ ;  $p = 9.2e-07$ ) and lumB ( $n = 407$ ;  $p =$

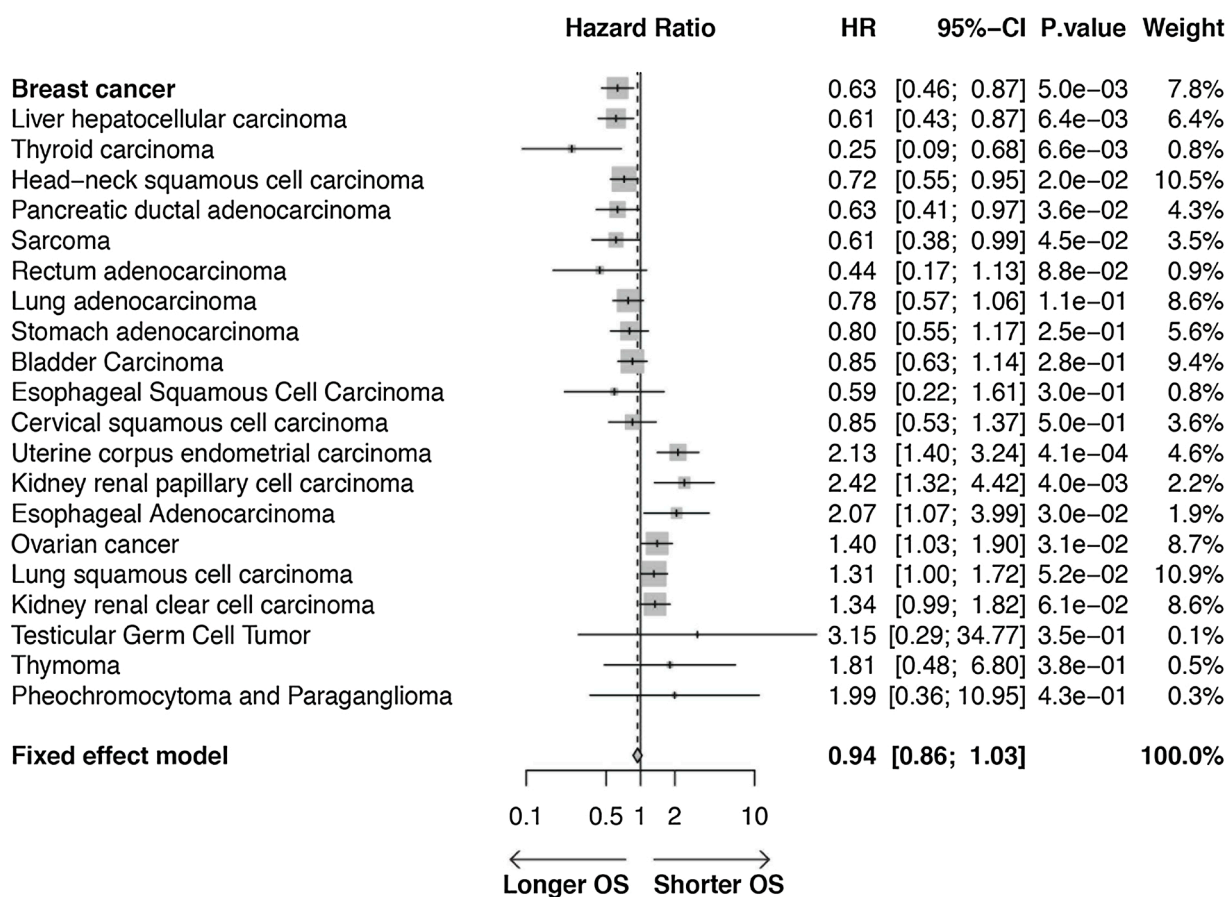


**Fig. 2.** Association between LINC01087 expression and OS in cancer patients. Forest plot of HR for OS assessed by cancer histotypes (BC highlighted in bold). The HRs were obtained from the Kaplan-Meier plotter. With the exception of breast cancer listed first for emphasis, tumors are ranked in ascending order of p-values. Horizontal lines represent CI. BC, breast cancer; CI, confidence interval; HR, hazard ratio; OS, overall survival.

0.0057) breast cancers (Fig. 3h, i). Similarly, an extended OS was witnessed in lumA BCs expressing a high level of LINC01087 ( $n = 271$ ;  $p = 0.0019$ ; Fig. 3j). Thus, survival curves demonstrated that high expression of LINC01087 was associated with better outcome in the luminal subtypes.

The hazard ratio (HR) value was lower in TNBC patients than in the lumA and lumB cohorts, with a significant 63, 52 and 35% lower risk of relapse, respectively, for tumors expressing higher levels of LINC01087 (Fig. 3d, h, i). Taking into account that normal breast tissue expresses an intermediate expression level of LINC01087 as compared to TNBC and luminal malignant tissues (Figs. 1b, c), LINC01087 seemed to be associated with a better prognosis in two distinct cellular environments. On one hand, higher expression of LINC01087 in TNBC brings its level closer to physiological levels, correlating with reduced aggressiveness of the disease. On the other hand, despite a constitutive overexpression of LINC01087 in luminal BCs, a further increase of its level was associated with better RFS.

Taken together, these multivariate analyses evidenced an association between a lower level of LINC01087 and a worsen outcome in all selected cohorts of both TNBC and luminal BC subtypes. Therefore, the altered expression level of LINC01087 could be considered as a prognostic biomarker in TNBC and luminal BC patients.

#### 4.4. LINC01087 deregulation is associated with molecular subtypes, independently of the histological or mutational status of breast cancer

To determine whether the modulated expression of LINC01087 could contribute to the development and/or progression of breast cancer, we investigated its association with common clinical parameters and the

histological origin of the tumor within the cohort of BC patients available in the TCGA database.

At first sight, we assessed the association between the level of expression of LINC01087 and clinicopathological features in BC patients of the TCGA database (e.g. age, gender, tumor stage and size). The size of the tumor appeared significantly associated with LINC01087 expression in the TCGA analysis (Supplementary Table S4). Moreover, a significant positive correlation between the expression of LINC01087 and hormone-related genes appeared. Indeed, LINC01087 was detected in PR-positive and ER-positive BCs but absent or strongly down-regulated in samples deficient for these hormone receptors (Supplementary Figure S4, Supplementary Table S4).

Regarding the histological parameters, the expression of LINC01087 appeared differentially regulated across the different breast tumor histotypes. Indeed, it was less abundant in aggressive and invasive metastatic carcinomas as compared to infiltrating ductal carcinomas or lobular carcinomas (adjusted p-values of 0.0038 and 0.00001, respectively; Fig. 4a).

However, by subdividing the most represented histological subtype, namely infiltrating ductal carcinoma, according to its molecular features (lumA, lumB or TNBC), when such information was available, we noticed a dichotomous clustering of the samples based on the expression profile of LINC01087. In details, within infiltrating ductal carcinomas, specimens expressing a high level of LINC01087 were almost exclusively luminal BCs, whereas tumors harboring low levels of LINC01087 appeared to be of the TNBC subtype (Fig. 4b).

Altogether, these data corroborated a predominant association between the downregulation of LINC01087 and the TNBC molecular subtype, as well as LINC01087 upregulation and the luminal subtypes,

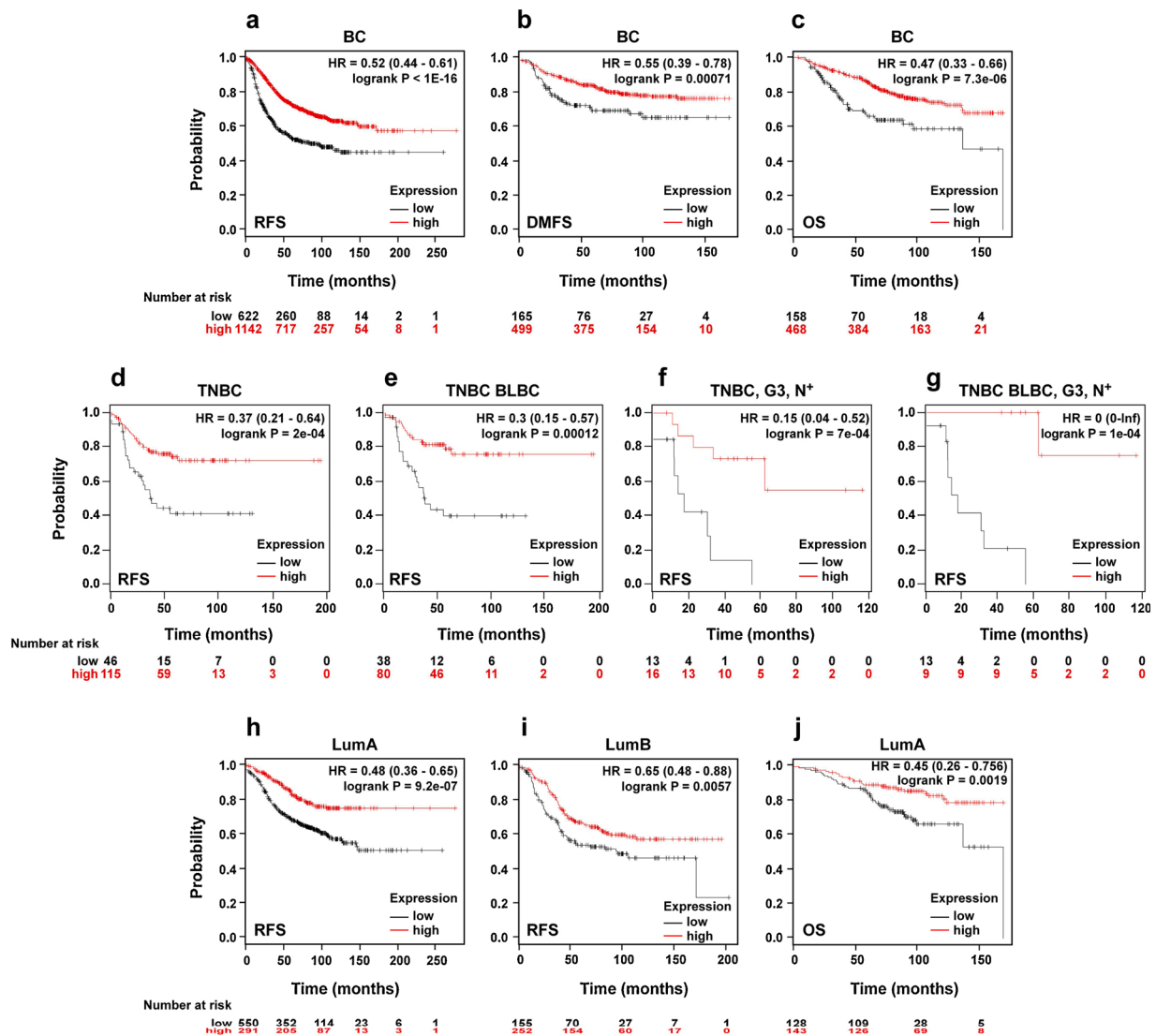


**Fig. 3.** The expression level of LINC01087 predicts survival of BC patients. Kaplan-Meier Plotter database was used to generate, by merging data from different datasets, the survival curves according to the level of expression of LINC01087. (a-c) Kaplan-Meier analysis of RFS (a), DMFS (b) and OS (c) of breast cancer patients expressing high (red curves) versus low (black curves) level of LINC01087. (d-e) RFS analyses for LINC01087 expression of TNBC breast cancer patients (d; n = 161; \*p = 2e-04) and, more specifically, in patients affected by a TNBC of basal intrinsic subtype (e; n = 118; \*p = 0.00012). (f-g) RFS analyses according to the expression level of LINC01087 in patients with advanced TNBC (grade 3 tumor, lymph node involvement) either without (f; n = 29; \*\*p = 7e-04) or with (g; n = 22; \*\*\*p = 1e-04) basal intrinsic features. (h-i) RFS analyses for LINC01087 expression of luminal A (h; n = 841; \*\*\*\*p = 9.2e-07) and luminal B (i; n = 407; \*\*p = 0.0057) breast cancer patients. (j) OS analysis for LINC01087 expression of luminal A breast cancer patients (n = 271; \*\*p = 0.0019). BC, breast cancer; BLBC, basal-like breast cancer subtype; DMFS, distant metastasis-free survival; G3, grade 3 tumor; N+, positive lymph node status; OS, overall survival; RFS, relapse-free survival; TNBC, triple-negative breast cancer.

independently of the histological nature of BC. Next, we investigated if the dysregulated expression of LINC01087 could be a prognostic indicator of BC aggressiveness. Considering the important role played by the detection test of *BRCA1/2* gene mutations in assessing the risk of BC development as well as its prognosis and therapy responsiveness, we analyzed the possibility that LINC01087 expression might vary depending on the mutational status of *BRCA1/2* [1,32]. Moreover, approximately 41% of BCs present a mutation in the gene *TP53* [1]. These *TP53* mutations have a negative prognostic value and are associated with an aggressive phenotype, such as TNBC, as well as with chemoresistance [33]. Therefore, we compared the expression of LINC01087 in BC patient samples harboring mutations in these three major tumor suppressors *BRCA1* (*BRCA1m*), *BRCA2* (*BRCA2m*) or *TP53* (*TP53m*) with a control arm carrying wild-type copies of these genes (*BRCA1wt*, *BRCA2wt*, *TP53wt*). This latter analysis revealed a significantly reduced expression of LINC01087 in BC patients bearing *BRCA1*

and *TP53* mutated tumors in comparison to wild-type samples. In contrast, no significant differences were observed for *BRCA2* (Fig. 4c,d).

To refine our analysis, we investigated the expression level of LINC01087 according to the mutational status of all three genes, rather than one single, at a time (Fig. 4e). In comparison to wild-type BC samples (Fig. 4c), the expression of LINC01087 was effectively weaker in BC patients bearing mutations of *TP53*, regardless of the *BRCA1* mutational status. In the absence of mutated *TP53*, neither *BRCA1* nor *BRCA2* mutations were associated with an aberrant expression of LINC01087 (Fig. 4e).

In the next step, we aimed at weighing the importance of the mutational status over the molecular subtype of BC on the regulation of LINC01087 expression. As we did for the histological data, when the information was available, we subdivided the largest cohort of patients with mutated tumor suppressors, namely BCs with a single mutation in *TP53* (i.e. *BRCA1wt* and *BRCA2wt*), based on their molecular features.



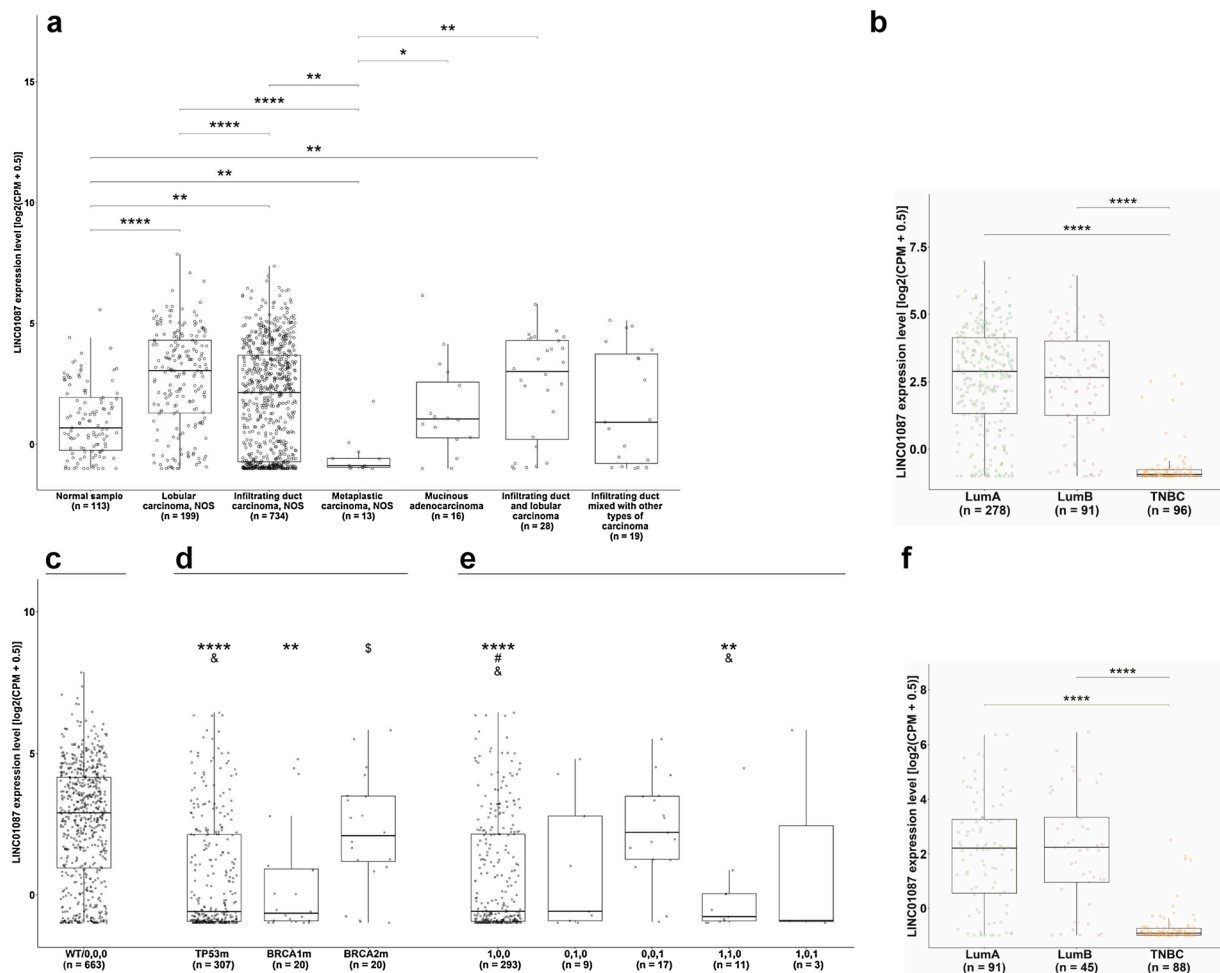


**Fig. 4.** The deregulation of LINC01087 segregates BC molecular subtypes, regardless of the histological and mutational status of BC. (a) Evaluation of LINC01087 expression in patients affected with different histological BC types. (b) Focus on the level of expression of LINC01087 in infiltrating ductal carcinomas based on BC molecular classification. (c-e) Representation of LINC01087 expression in BC patients harboring tumors with wild-type (wt) or mutant (m) versions of the tumor suppressors *TP53*, *BRCA1*, and *BRCA2*. (c) Wild-type controls: WT/0,0,0 = *TP53*wt, *BRCA1*wt, *BRCA2*wt. (d) *TP53*m = *TP53* mutated tumors (regardless of the mutational status of *BRCA1*&2); *BRCA1*m = *BRCA1* mutated (regardless of *TP53* & *BRCA2* mutations); *BRCA2*m = *BRCA2* mutated (regardless of *TP53* & *BRCA1* mutations). (e) 0,0,1 = *TP53*wt, *BRCA1*wt, *BRCA2*m; 0,1,0 = *TP53*wt, *BRCA1*m, *BRCA2*wt; 1,0,0 = *TP53*m, *BRCA1*wt, *BRCA2*wt; 1,0,1 = *TP53*m, *BRCA1*wt, *BRCA2*m; 1,1,0 = *TP53*m, *BRCA1*m, *BRCA2*wt. Of note, other combinations of mutations were not observed among the cohorts available. (f) LINC01087 expression in *TP53*m tumors subdivided according to their molecular subtype. The level of LINC01087 expression is reported as  $\log_2(\text{CPM} + 0.5)$  for each patient's BC sample extracted from both TCGA and cBioPortal databases. (c-e) Symbols indicate significant changes with respect to WT/0,0,0 (wild-type controls) (\*\* $p \leq 0.01$ , \*\*\*\* $p \leq 0.0001$ ), or to *TP53*m ( $\#p \leq 0.05$ ), or to *BRCA2*m ( $\$p \leq 0.05$ ), or to 0,0,1 (*TP53*wt, *BRCA1*wt, *BRCA2*m) ( $\&p \leq 0.05$ ) samples. BC, breast cancer; CPM, counts per million; duct, ductal; LumA, luminal A; LumB, luminal B; NOS, not otherwise specified; TNBC, triple-negative breast cancer.

Once again, within *TP53*m BC patients, LINC01087 was barely expressed in TNBC, whereas its level was higher in the luminal A and B subtypes (Fig. 4f). Thus, despite the presence of mutations in genes affiliated with tumor aggressiveness, the level of LINC01087 expression was still segregating TNBC and luminal cancers.

In conclusion, these findings highlight the potential value of LINC01087 downregulation for diagnosing TNBCs and its upregulation for the diagnosis of luminal molecular subtypes, regardless of the clinicopathological parameters, histological nature and *TP53/BRCA1/2* mutational status of BC.

#### 4.5. In silico analysis of the molecular and cellular impact of LINC01087 in TNBC

Although the number of annotated lncRNAs is ever-expanding, most of them still have unclear biological functions. They have been involved in chromatin remodeling and regulatory activities at the epigenetic, transcriptional and post-transcriptional levels. Consequently, their deregulation could contribute to oncogenesis [13]. LINC01087

(Ensembl ID: ENSG00000224559) is an intergenic lncRNA whose gene spans over 12.591 bp on the 2q21.1 chromosome and contains two exons (exon 1: 2.154 bp; exon 2: 1.362 bp) and one intron of 9.075 bp. In physiological conditions, its detection is restricted to the breast and testis (GTEx expression data) (Supplementary Figure S5). Thus, we could not exclude that its deregulation impacts breast carcinogenesis and tumor aggressiveness. This hypothesis is supported by the intimate relationship that we uncovered between LINC01087 downregulation and the poor prognosis TNBC subtype, as well as its upregulation and a better clinical outcome in luminal BCs.

In order to get insights into the putative functions of LINC01087 in BC aggressiveness, we first compared the transcriptomic profile of TNBC samples expressing intermediate level of LINC01087 (TNBC LINC01087<sup>int</sup>) versus the specimens harboring the weakest expression of this lncRNA (TNBC LINC01087<sup>lo</sup>). The cut-off applied to segregate LINC01087<sup>lo</sup> and LINC01087<sup>int</sup> was 0.0242 CPM (corresponding to a  $\log_2[\text{CPM} + 0.5]$  value of -0.93).

Forty-three genes appeared significantly regulated (i.e.  $p\text{-value} \leq 0.05$ ,  $\log_2\text{FC} \geq |0.585|$ ) and were all positively associated with

LINC01087 expression in TNBC (Supplementary Figure S6a). Out of the 10 most upregulated genes, three had been attributed tumor suppressive functions in malignant tissues: *TMEFF2*, *TFE1*, and *NEFM* (respective log<sub>2</sub>FC of 3.98, 3.84, and 3.05; Supplementary Figure S6b) [34–36].

Furthermore, we analyzed the biological activity of these 43 genes associated with LINC01087 expression in TNBCs by conducting Gene Ontology (GO), Kyoto Encyclopedia of Genes and Genomes (KEGG) and REACTOME functional annotation and enrichment analyses. The 3 largest clusters of genes were tagged with the GO terms “protein binding”, “membrane”, and “integral component of membrane” (Fig. 5a, Supplementary Tables S5–S7). Ten genes were shared among these 3 clusters. They encoded 9 plasma membrane-bound proteins *CNTNAP2*, *DSCAML1*, *IGSF9B*, *KLHDC7A*, *LRFN2*, *NSG1*, *SLC9A3*, *TMEFF2* and *TMPRSS6*, together with *CLGN*, which is mostly detected in the nucleus

and endoplasmic reticulum (ER) (genecards.org). Of note, *NSG1* is not only enriched at the plasma membrane but can be found in the nucleus, ER, Golgi apparatus, endosome and lysosome. *CNTNAP2*, *DSCAML1*, *SLC9A3*, *TMEFF2* and *TMPRSS6* are also detected in the extracellular milieu (genecards.org).

Additionally, a gene ontology enrichment analysis revealed an over-representation of DE genes involved in the “transport of inorganic cations/anions and amino acids/oligopeptide” and encoding the solute carrier (SLC) membrane transporters *SLC9A3*, *SLC4A9*, and *SLC17A8* (Fig. 5b, Supplementary Table S8).

Finally, to further deepen the biological processes related to LINC01087, we mapped the protein-protein interaction (PPI) network of 19 out of the 43 candidate genes (in bold in Supplementary Table S5) belonging to the largest (≥ 20 genes) GO annotated clusters (Fig. 5a). The assay was performed using the Search Tool for the Retrieval of

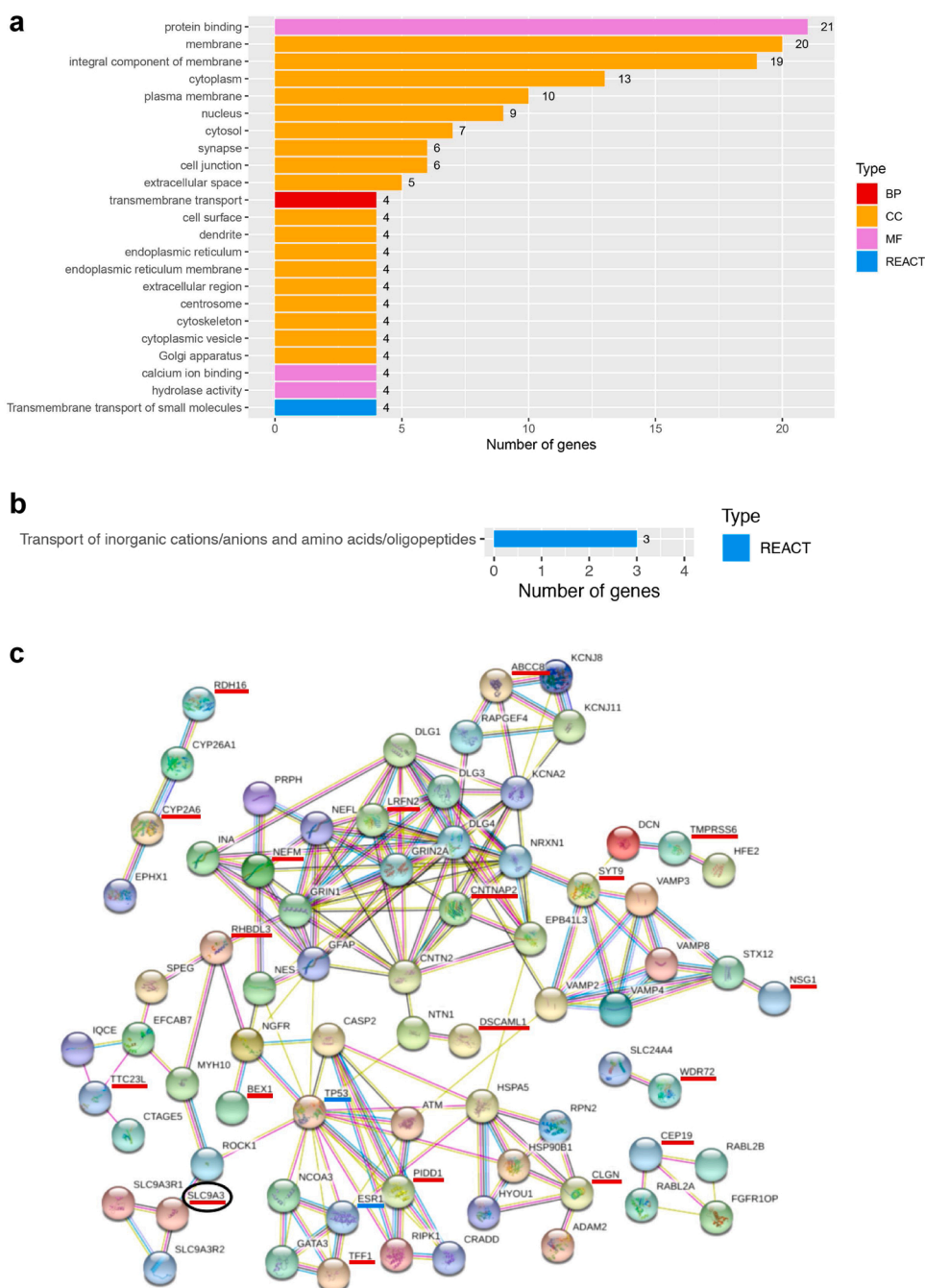


**Fig. 5.** Biological functions and interaction network of some factors whose expression is positively correlated with LINC01087 in TNBC. (a, b) Bar graphs display the main ontology terms attributed to the 43 genes whose expression was positively correlated with LINC01087 level in TNBCs according to GO, KEGG, and REACTOME gene annotation (a) and enrichment (b) analyses. Panel a illustrates the annotated clusters of at least 4 genes (see Supplementary Tables S5 to S7 for details). Panel b displays the only gene ontology annotation that was significantly enriched (see Supplementary Table S8 for details). Sub-categories of the GO hierarchy are color-coded: “Biological process” [BP] in red; “Cellular component” [CC] in orange; “Molecular function” [MF] in fuchsia. REACTOME gene ontology (REACT) is in blue. (c) PPI network established using STRING database. Nodes represent proteins while experimentally validated PPIs are represented by edges. Input data (underlined in red) consisted of proteins whose corresponding gene belonged to GO annotated clusters of ≥ 20 members (panel a) and present in the STRING database. The protein attributed to the significantly enriched ontology term (panel b) is circled in black (i.e. *SLC9A3*). Some proteins known to intervene in breast carcinogenesis are underlined in blue (i.e. *TP53*, *ESR1*). GO, gene ontology; KEGG, Kyoto encyclopedia of genes and genomes; PPI, protein-protein interaction; STRING, search tool for the retrieval of interacting genes/proteins; TNBC, triple-negative breast cancer.

Interacting Genes/Proteins (STRING) online database. The resulting map confirmed strong interconnections between 15 of these proteins mostly associated with (a) cell survival (e.g. PIDD1, TFF1); (b) cell cycle, proliferation and differentiation (e.g. BEX1, TMEFF2, TTC23 L), (c) transporter activity (e.g. ABCC8, CYP2A6, SLC9A3, SYT9), or (d) cell adhesion and extracellular matrix (ECM) remodeling (e.g. CNTNAP2, DSCAML1, LRFN2, NEFM, TMPPRS6) (Fig. 5c).

Taken together, these results suggested that LINC01087 might stimulate the expression of factors mostly located at cell and organelle membranes and responsible for sensing, exchanging with, and remodeling the extracellular milieu. Several of these targets are known tumor suppressors, which could explain a better prognosis of TNBCs harboring higher level of LINC01087.

#### 4.6. *In silico* analysis of the molecular and cellular impact of LINC01087 in luminal BC

Next, we repeated the *in silico* analyses on luminal BC samples of the TCGA database in order to consolidate our findings on the influence of LINC01087 on BC tumorigenesis.

First, we determined the transcriptional imprint that distinguishes luminal BCs expressing a high level of LINC01087 (Lum LINC01087<sup>hi</sup>) from the specimens harboring an intermediate level (Lum LINC01087<sup>int</sup>). The cut-off value applied to segregate LINC01087<sup>int</sup> from LINC01087<sup>hi</sup> was computed at 3.331 CPM, corresponding to a  $\log_2(\text{CPM} + 0.5)$  value of 1.93 (Fig. 1c).

A total of 345 genes in lumA and 30 genes in lumB emerged as significantly modulated (i.e.  $\log_2\text{FC} \geq |0.585|$ ,  $p\text{-value} \leq 0.05$ ) upon LINC01087 overexpression (Supplementary Figure S6 and Supplementary Tables S9, S10). The elevated number of DE genes in lumA BC was unexpected and might reflect cellular heterogeneity within each individual lumA BC tissue and/or between specimens recorded in the TCGA database.

Nonetheless, some concordant results were observed between TNBC and lumA BC. Indeed, two genes were upregulated in both TNBC and lumA BC upon variations of LINC01087 expression, namely SYT9 encoding the calcium-binding synaptotagmin 9, and ANKRD30B encoding ankyrin repeat domain 30B, a breast cancer antigen. Additionally, some families of modulated genes with well-defined structural and/or functional characteristics were represented in the two BC subtypes: cytochromes P450 ( $\uparrow\text{CYP2A6}$ ,  $\uparrow\text{CYP3A4}$ ,  $\uparrow\text{CYP3A7}$ ), solute carriers ( $\uparrow\text{SLC17A8}$ ,  $\uparrow\text{SLC9A3}$ ,  $\uparrow\text{SLC4A9}$ ,  $\uparrow\text{SLC6A4}$ ,  $\uparrow\text{SLC16A6}$ ,  $\downarrow\text{SLC6A12}$ ,  $\downarrow\text{SLC15A1}$ ,  $\downarrow\text{SLC38A3}$ ,  $\downarrow\text{SLC28A1}$ ), tetratricopeptide repeat domain-containing factors ( $\uparrow\text{TTC6}$ ,  $\uparrow\text{TTC23 L}$ ,  $\uparrow\text{TTC34}$ ) and Kelch domain-containing proteins ( $\uparrow\text{KLHDC7A}$ ,  $\downarrow\text{KLHDC8A}$ ). Although LINC01087 function remains undetermined to date, these similarities may point toward a series of genes intimately regulated by this lncRNA (Supplementary Figure S6, Supplementary Table S9).

Similarities of transcriptional profiles were also observed between the two luminal BC subtypes. In particular, we noticed a positive link between the level of LINC01087 and the expression of different members of the multigene family POTE. Precisely, POTEH, and POTEI were upregulated in both LINC01087<sup>hi</sup> lumA and lumB BCs, while POTEJ, POTEK, POTEF, POTEH and POTEI were found overexpressed only in LINC01087<sup>hi</sup> lumA samples (Supplementary Figure S6, Supplementary Tables S9, S10). This family regroups poorly investigated cancer/testis antigens [37,38]. Moreover, a decreased expression of some S100 genes was witnessed upon LINC01087 upregulation: S100A8 and S100A9 in lumA BC and S100A7 in lumB samples (Supplementary Tables S9, S10). These extracellular factors regulate various biological processes including apoptosis, cell proliferation, adhesion, or leukocyte migration [39]. Other genes modulated upon LINC01087 upregulation in luminal BCs have been associated with breast carcinogenesis such as MSLN, CAMP, RARRES1, and CPA4 [40–43]. The expression of MSLN was strongly reduced in LINC01087<sup>hi</sup> lumA BCs ( $\log_2\text{FC} = -2.7$ ; Supplementary Figure S6c, Supplementary Table S9), whereas CAMP,

RARRES1, and CPA4 showed negative regulation in LINC01087<sup>hi</sup> lumB BCs ( $\log_2\text{FC} = -3.4$ ,  $-2.2$ , and  $-1.66$ , respectively; Supplementary Figure S6d, Supplementary Table S10).

Finally, we proceeded to GO, KEGG and REACTOME functional annotation analyses on the 100 most up- and down-regulated genes in lumA and lumB BCs. In accordance with the results obtained for TNBC, a majority of genes differentially expressed between LINC01087<sup>hi</sup> and LINC01087<sup>int</sup> luminal BC samples clustered under the ontology annotation “protein binding”, indicating their integration into protein complexes (Fig. 6a, Fig. 7a, Supplementary Tables S11–S13).

In both lumA and lumB BCs, an enrichment analysis highlighted a predominance of factors ascribed to the “extracellular region” among the genes whose expression varied with LINC01087 upregulation. (Fig. 6b, Fig. 7b, Supplementary Tables S14 and S15).

These sets of genes included the aforementioned factors related to breast carcinogenesis, namely CAMP, CPA4, RARRES1, S100A7 in lumB specimens and MSLN in lumA BC, among others (Supplementary Tables S14).

Furthermore, a significant enrichment in clusters of genes assigned to immune functions, mostly innate immunity, was uncovered in lumA and lumB BCs (Fig. 6b, Fig. 7b, Supplementary Tables S14, S15). In lumA BC, these clusters regrouped S100A8, S100A9, the genes encoding the transcription factor FOSL1 ( $\log_2\text{FC} = -0.97$ ), the chemokine CCL7 ( $\log_2\text{FC} = -0.91$ ) and the matrix metalloproteinase MMP1 ( $\log_2\text{FC} = -1.28$ ). In lumB BC, they regrouped S100A7 and CAMP which encodes the antimicrobial peptide cathelicidin (Supplementary Tables S14, S15). All these genes have been involved in breast tumorigenesis [44–49].

Exclusively in lumA BC, 14 “biological processes” were significantly enriched across the plethora of genes modulated upon upregulation of LINC01087. These biological processes regroup more than 80 genes involved in tissue development and cell differentiation, including the aforementioned MSLN, FOSL1, or S100 and SLC genes (Fig. 7b, Supplementary Tables S14, S15). Furthermore, we evidenced an enrichment in clusters of genes related to the G protein-coupled receptor (GPCR) signaling pathway. It included GNRHR, which encodes the receptor of the gonadotropin-releasing hormone (GNRH) (Fig. 7, Supplementary Tables S13–S15). GNRHR was significantly up-regulated in LINC01087<sup>hi</sup> lumA BCs ( $\log_2\text{FC} = 1.07$ ), exhibiting a positive correlation with LINC01087 (Supplementary Table S9). Interestingly, GPCRs play a critical role in the initiation and progression of hormone-refractory BC [50]. In this line, certain drugs targeting GPCRs have been designed for BC treatment [51]. Goserelin is a GNRH agonist indicated for endocrine therapy of pre-menopausal woman affected by ER<sup>+</sup> luminal BCs [51]. Considering the favorable input of LINC01087 on the prognosis of BC, its upregulation could reduce the aggressiveness of ER<sup>+</sup> luminal BC by sensitizing the tumor to GNRH through increased production of its receptor. Finally, upregulation of LINC01087 coincided with an enrichment of genes belonging to the hypoxia-inducible factor pathway (Fig. 7b, Supplementary Table S15). This pathway is commonly involved in cancer progression, angiogenesis, metastasis and resistance to therapy [52]. The two genes falling into this cluster, namely CA9 and EPO which respectively encode the carbonic anhydrase IX and erythropoietin, were downregulated in LINC01087<sup>hi</sup> lumA BC samples ( $\log_2\text{FC} = -1.72$  and  $-1.71$ , respectively) (Supplementary Table S9). Therefore, as both EPO and CA9 are protumoral factors, their decreased expression upon LINC01087 upregulation provides further clues in favor of a tumor suppressor activity of this lncRNA [53–56].

At last, PPI network analyses were carried out on the genes that were modulated upon upregulation of LINC01087, and that were affiliated with annotated clusters of  $\geq 5$  genes for lumB and  $\geq 20$  genes for lumA BC samples (Figs. 6c and Fig. 8).

In both luminal subtypes, the majority of the genes organized themselves within one large network of physical interactions at the protein level, with only a limited number of candidates isolated in satellite PPI networks (Figs. 6c and Fig. 8).

In the lumB subtype emerged a network of proteins responsible for

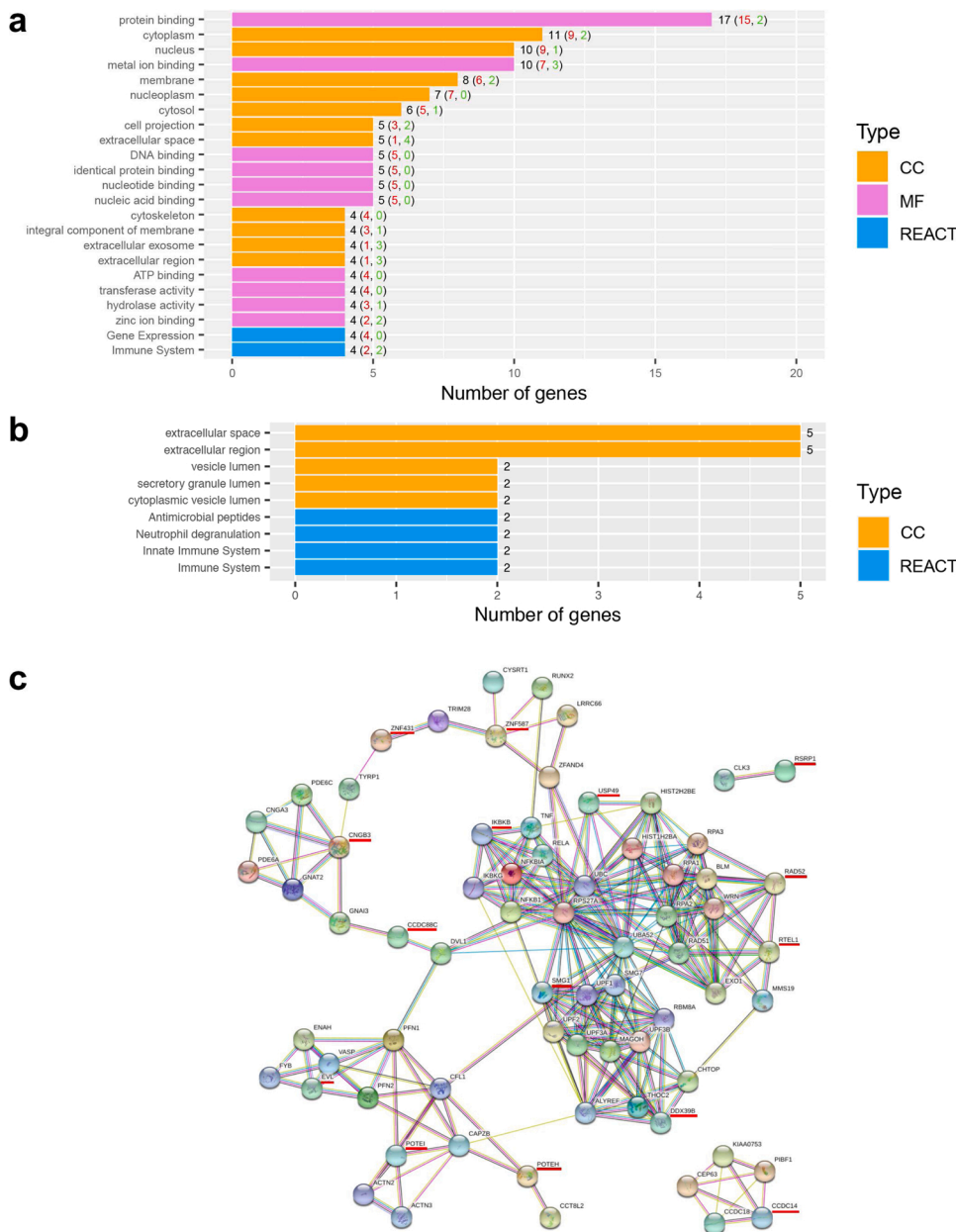


**Fig. 6.** Biological functions and interaction network of some factors whose expression varies along LINC01087 deregulation in luminal B BC. (a, b) Bar graphs display the main ontology terms attributed to the 30 genes that were differentially expressed between LINC01087<sup>hi</sup> and LINC01087<sup>int</sup> luminal B BC samples, according to GO, KEGG and REACTOME gene annotation (a) and enrichment (b) analyses. Panel a illustrates the annotated clusters that included  $\geq 4$  genes (see Supplementary Tables S12 and S13 for details). Panel b displays gene ontology annotations that were significantly enriched (see Supplementary Table S14 and S15 for details). Panels a and b indicate the total number (written in black) of genes allocated to each ontology annotation. Panel a also indicates the number of genes up- or down-regulated in red and green, respectively. Sub-categories of the GO hierarchy are color-coded: “Biological process” [BP] in red; “Cellular component” [CC] in orange; “Molecular function” [MF] in fuchsia. REACTOME gene ontology (REACT) is in blue. (c) PPI network established using STRING database. Nodes represent proteins while experimentally validated PPIs are represented by edges. Five interactants were displayed in the network per selected protein. Input data (underlined in red or green if up- or down-regulated, respectively) consisted of proteins whose corresponding gene belonged to GO annotated clusters of  $\geq 5$  members (panel a) and present in the STRING database. BC, breast cancer; GO, gene ontology; KEGG, Kyoto encyclopedia of genes and genomes; PPI, protein-protein interaction; STRING, search tool for the retrieval of interacting genes/proteins.

monitoring genome integrity and expression, such as DDX39A, RAD52, RTEL1, SMG1 and the zinc finger proteins ZNF431 and ZNF587. This first network appeared intimately connected with the NF- $\kappa$ B signaling pathway (including IKKBK) that plays a critical role in regulating cell viability and inflammation (Fig. 6c).

In the lumA subtype, a core network of inflammation-related factors included some components of the NF- $\kappa$ B signaling cascade (e.g. NFKB1, NFKBIZ), chemoattractants (e.g. CCL7, S100A8/A9), as well as chemokine and pattern recognition receptors (e.g. CCR2, CXCR4, MYD88, TLR10, NLRP8) (Fig. 8). This network appeared closely connected with elements of the response to hypoxia (e.g. CA9, EPO) or involved in cell proliferation and adhesion including the Wnt/ $\beta$ -catenin pathway (e.g. WNT3A, WNT5B, FZD1, FZD9, ACAN, NCAM1). Remarkably, components of these oncogenic networks were mostly downregulated at the transcriptional level when the levels of LINC01087 increased (Fig. 8).

Collectively, despite distinct malignant microenvironments between BC subtypes, these results obtained in luminal BCs supported the observations made in TNBC whereby LINC01087 upregulation would improve clinical outcome through transcriptional interference with

factors promoting breast carcinogenesis.

## 5. Discussion

Considering the negative impact that the heterogeneity of BC exerts on the clinical decision making, there is an urgent need for identifying specific biomarkers allowing to easily and precisely distinguish between the different BC subtypes [1,10].

In the last decade, cumulative studies emphasized the functional relevance of lncRNAs in breast cancer and proposed their consideration to classify the heterogeneous collection of BC subtypes [19]. These findings have provided knowledge on the regulatory mechanisms that drive breast tumorigenesis [13,22]. In the routine clinical research and practice, the perturbation of lncRNAs expression has raised consideration for improving the care of BC. Therefore, we first applied a high-throughput sequencing approach, followed by bioinformatics analyses in order to define a specific signature of lncRNAs in the different BC subtypes. Among all the lncRNAs identified, we focused our attention on a strongly modulated intergenic lncRNA named LINC01087, which

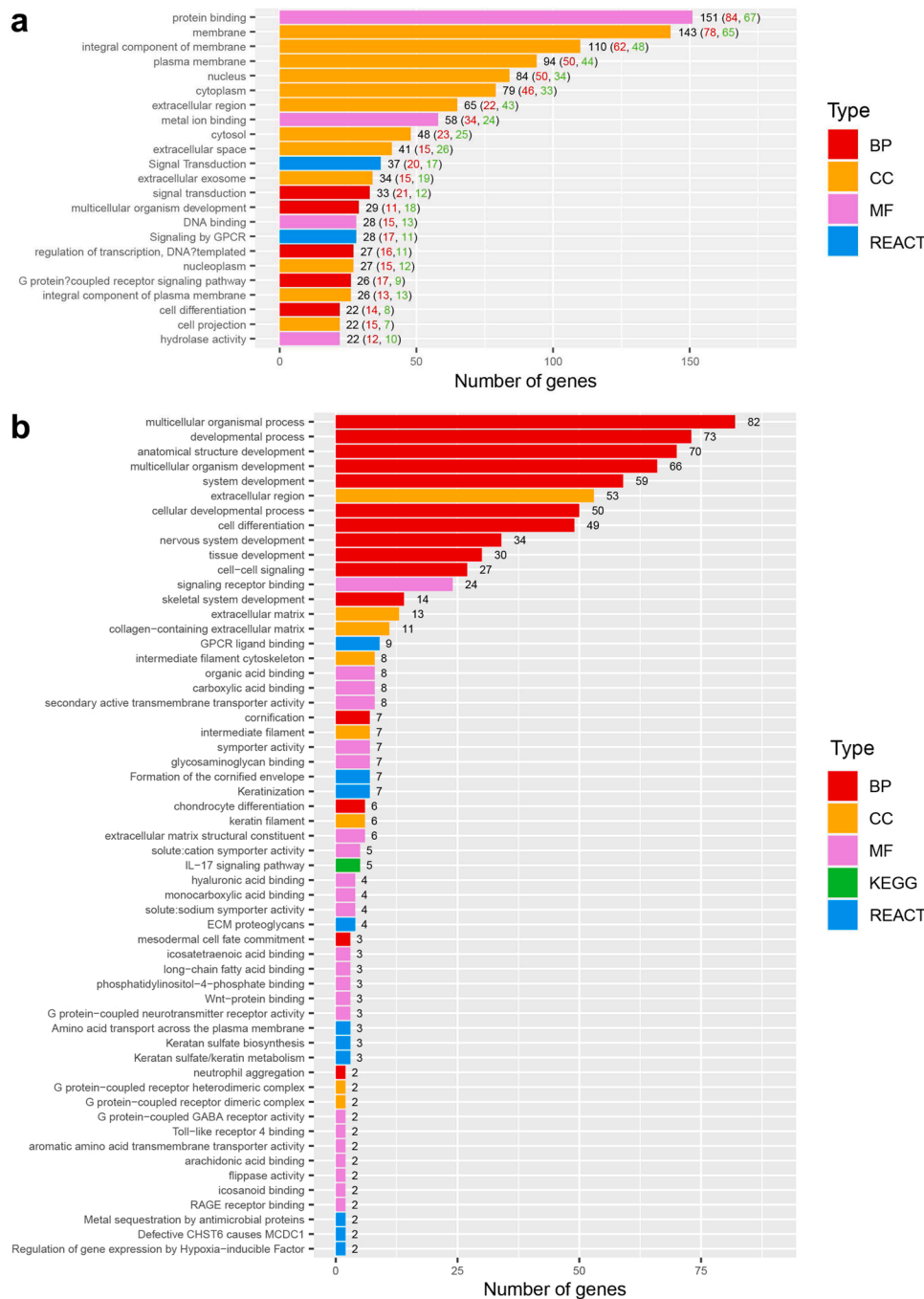


**Fig. 7.** LINC01087 biological functions in luminal A BCs. (a, b) Bar graphs display the main ontology terms attributed to the 345 genes that were differentially expressed between LINC01087<sup>hi</sup> and LINC01087<sup>int</sup> luminal A BC samples, according to GO, KEGG and REACTOME gene annotation (a) and enrichment (b) analyses. Panel a illustrates the annotated clusters that included  $\geq 22$  genes (see Supplementary Tables S11 and S13 for details). Panel b displays gene ontology annotations that were significantly enriched (see Supplementary Tables S14 and S15 for details). Panels a and b indicate the total number (written in black) of genes allocated to each ontology annotation. Panel a also indicates the number of genes up- or down-regulated in red and green, respectively. Subcategories of the GO hierarchy are color-coded: Red, GO Biological process terms [BP]; Orange, GO Cellular component terms [CC]; Fuchsia, GO Molecular function terms [MF]; Green, KEGG pathways; Blue, REACTOME [REACT] pathways). GO, Gene ontology; KEGG, Kyoto Encyclopedia of Genes and Genomes.

had been under-investigated so far.

In the present study, we described a deregulated expression of LINC01087 as a diagnostic and prognostic biomarker for TNBC and luminal BCs. In both RNA-sequencing and bioinformatics analyses, LINC01087 was weakly expressed in TNBC patient samples and highly expressed in luminal samples as opposed to normal specimens. Such differential expression between TNBC and luminal subtypes has been validated *in vitro* and *in silico* in breast cancer cell lines. Our observation concerning LINC01087 deregulation in BCs has been comforted by contemporary investigations [57,58].

The clinical behavior of TNBCs remains difficult to predict. Generally, TNBCs have the worst clinical outcome and highest rate of recurrence within the first 5 years that follow diagnosis [1,59]. Efforts are being made to identify some biomarkers that could stratify patients into subgroups with low *versus* high risk of recurrence and short- *versus*

long-term survival. Thus, the potential prognostic value of LINC01087 was studied using the Kaplan-Meier plotter online database. The survival curves showed that a down-expression of LINC01087 was substantially correlated with a lower RFS in TNBC patients, especially in advanced stages characterized by a lymph node involvement and a high-grade tumor. Thus, quantitative detection of LINC01087 may be clinically useful for the diagnosis and monitoring of the TNBC subtype and its gradation and, consequently, as a prognostic biomarker in TNBC patients.

The same considerations also referred to the luminal BCs that generally have a better prognosis compared to the TNBCs [1]. Following interrogation of the KMplot database, we reported that high levels of LINC01087 correlated with extended RFS in both luminal A and B cohorts, as well as prolonged OS in luminal A patients.

The deregulated expression of LINC01087 appeared specific of the

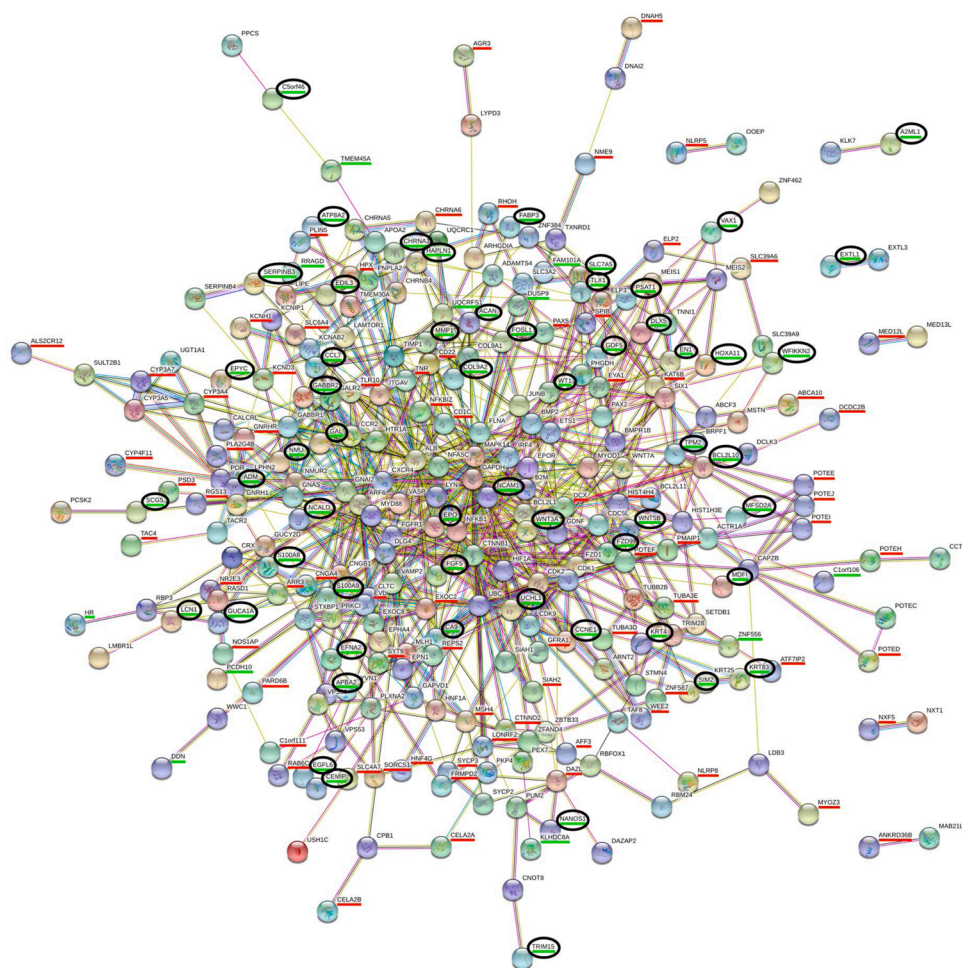


**Fig. 8.** Protein-protein interaction network of some factors whose expression varies along LINC01087 deregulation in luminal A BC. PPI network established using STRING database. Nodes represent proteins while experimentally validated PPIs are represented by edges. Input data consisted of proteins whose gene (i) was significantly modulated (underlined in red or green if up- or down-regulated, respectively) between LINC01087<sup>hi</sup> and LINC01087<sup>int</sup> luminal A BC samples, (ii) belonged to GO annotated clusters of  $\geq 20$  members, and (iii) was present in the STRING database (see Fig. 7, Supplementary Tables S9, S11, S13). Five interactants were displayed in the network per selected protein. Proteins attributed to significantly enriched ontology terms are circled in black (see Supplementary Table S14). BC, breast cancer; GO, gene ontology; PPI, protein-protein interaction; STRING, Search tool for the retrieval of interacting genes/proteins.

BC subtype, thus offering an opportunity to distinguish between luminal BCs and TNBCs. Moreover, the expression of LINC01087 seemed to exhibit tumor suppressive properties, allowing to predict a better survival in BC subtypes. Additionally, ROC curves confirmed the diagnostic value of LINC01087 for TNBC as well as lumA and lumB BCs. Thus, the level of LINC01087 expression within the tumor might have both diagnostic and prognostic utility.

BC is a complex genetic disease that shows a high prevalence of *TP53* mutations, particularly in TNBCs [1]. Detection of alterations in *TP53* is considered as a negative prognostic factor due to its association with more aggressive BC subtypes when compared to BC subjects who possess wild-type copies of *TP53* [60]. In addition, BC patients that harbor *TP53* mutations can carry alterations in the genes *BRCA1* or *BRCA2*, thus increasing cancer aggressiveness [61]. Therefore, to evaluate the impact of LINC01087 on BC prognosis, we measured its level of expression according to the mutational status of *BRCA1* and *BRCA2*, as well as to that of *TP53*. Interestingly, we noticed a significant decrease of LINC01087 in *TP53*-mutated specimens, together with a similar trend in *BRCA1*-mutated ones. Nevertheless, these correlations ultimately depended on the TNBC molecular subtype, which is naturally enriched in the samples mutated for *TP53* and/or *BRCA1*. In this line, *TP53* mutated BC patients harboring high levels of LINC01087 belonged to luminal subtypes. Altogether, these results comforted that the expression level of LINC01087 can determine the molecular subtype of BC, independently of its mutational status.

Prospective clinical studies gathering a larger number of patients and covering the different clinicopathological, histological and mutational subtypes of BC will be required to consolidate our findings on the diagnostic and prognostic value of a downregulated LINC01087 in

TNBC, as well as of an upregulated LINC01087 in luminal BCs.

In the scenario of a potential role of LINC01087 in breast carcinogenesis and cancer aggressiveness, we initiated some *in silico* investigations to characterize the molecular and cellular processes that LINC01087 may regulate in both TNBC and luminal BC. First, we performed a comparative analysis of the transcriptomic profiles of TNBC samples harboring intermediate *versus* low level of LINC01087, and of luminal BC samples harboring high *versus* intermediate level of LINC01087. In this setting, intermediate expression of LINC01087 corresponds to its level in normal breast tissue. Such comparisons within each individual BC subtypes, rather than between normal and malignant tissues, limit transcriptomic bias caused by oncogenic aberrations. They allowed the identification of genes differentially expressed along variation of LINC01087 expression. Next, we investigated the biological functions of these genes thanks to gene ontology annotation and enrichment analyses. Finally, we deepened our functional study by modeling the protein-protein interaction network of the main annotated and enriched clusters of DE genes.

This work uncovered a transcriptional signature of individual factors and families of proteins that underwent modulation upon enhanced expression of LINC01087 in both TNBC and lumA subtypes. This imprint consisted of an upregulation of *SYT9*, *ANKRD30B*, several cytochromes *P450* and *TTC* factors, and of mixed regulations of *SLC* solute carriers and of *KLHDC* proteins. Moreover, we reported some homologies between the transcriptomic profiles of LINC01087<sup>hi</sup> lumA and lumB BCs. In particular, various members of the *POTE* and *S100* families showed up- and down-regulation, respectively, in both luminal subtypes. Also, LINC01087 upregulation coincided with modulations of inflammation-related genes, including *S100* proteins, in the two luminal subtypes.

Collectively, these (families of) genes shared between BC subtypes would represent putative molecular targets of LINC01087, supporting its apparent tumor suppressive activity. Although the function of most of these targets remains poorly understood, particularly in breast cancer, some of them have been involved in breast carcinogenesis.

Cytochromes P450 are enzymes achieving multiple functions such as the oxidation of lipids, steroids, and drugs [62,63]. Alteration of expression or activity of *CYP2A6* impacts cancer incidence and resistance to chemotherapy, notably in BC [62]. In TNBC, we observed a positive correlation between the levels of *CYP2A6* mRNA and LINC01087.

S100 proteins promote cancer by stimulating cell proliferation, dissemination, and angiogenesis [39]. Thus, overexpression of *S100A7*, *A8* and *A9* has been associated with tumor aggressiveness, metastasis and a poor prognosis in ER- BC when compared to ER<sup>+</sup> BC [39]. Concerning *S100A7*, it displays a contrasting role according to the ER status, acting as a tumor suppressor gene in ER<sup>+</sup> BCs and as an oncogene in ER-BCs [39]. Also, *S100A7*, *S100A8* and *S100A9* play a decisive role in igniting inflammation and favoring immune evasion [39]. In this line, the expression of *S100A9* in ER- PR- BCs induces inflammatory cytokines and is associated with unfavorable OS [64]. In the present work, gene expression of *S100A8* and *S100A9* (forming the calprotectin), and of *S100A7* (also known as psoriasin), was attenuated upon upregulation of LINC01087 in lumA and lumB BCs, respectively.

On top of *S100s*, upregulation of LINC01087 interfered with a plethora of immune-related genes in both luminal BC subtypes. For instance, *IKKBK* encoding a component of the NF- $\kappa$ B signaling pathway, as well as *CAMP* and *LY6G5B* (*lymphocyte antigen 6 family member G5B*) were differentially expressed in lumB BC. Conversely in lumA BC, overexpression of LINC01087 modulated the level of other components of the NF- $\kappa$ B signaling cascade (e.g. NFKB1, NFKBIZ) and of the chemokine CCL7 and some pattern recognition receptors like TLR10 and NLRP8, among others. Considering the well-accepted contribution of inflammation to cancer initiation and progression and, by contrast, of cancer immunosurveillance in eliminating malignant entities, LINC01087-mediated control of pro- and anti-inflammatory molecules could impact breast carcinogenesis [65,66].

Moreover, variation of the level of LINC01087 in the different BC subtypes coincided with a modulated expression of factors (mostly secreted) regulating genome integrity and expression, cell survival, cell proliferation, or again cell adhesion and invasion. Some of them have documented implication in breast carcinogenesis and will be presented below.

Cell survival is, at least partially, under the control of the NF- $\kappa$ B pathway [67]. As abovementioned, components of this signaling cascade appeared modulated upon expression of LINC01087 in both lumA and lumB BCs. In TNBC, PIDD1 (p53-induced death domain protein 1) was upregulated in LINC01087<sup>hi</sup> samples. PIDD1 interacts with caspase 2 to regulate apoptosis [68]. PIDD1 is associated with breast cancer cell survival, and its overexpression induces apoptosis in TP53-deficient tumor cells [69]. The gene *TFF1* (trefoil factor 1) underwent a remarkable increase in TNBC samples expressing a higher level of LINC01087. This gene exhibits lower expression in TNBC as compared to non-TNBC [70]. In particular, its expression relies on the status of the hormonal receptor, due to the presence of an ER response element in its promoter region [34,71]. In preclinical murine models, deficiency in *TFF1* increased breast cancer cell tumorigenicity and the development of mammary tumors [34]. A role for *TFF1* in TP53-mediated apoptotic process has been described through downregulation of miR-504 in gastric cancer. Another report defined a tumor-suppressor role of *TFF1* via the activation of the TP53/caspase pathway and the downregulation of miR-18a in retinoblastoma [72,73]. In the clinic, *TFF1* expression correlated with a favorable survival in BC [70].

Cell proliferation and adhesion is notably controlled by the Wnt/ $\beta$ -catenin pathway which is remarkably activated in breast cancers [74,

75]. In LINC01087<sup>hi</sup> lumA BCs, we found a downregulated expression of WNT3A, WNT5B and FZD9, which integrate this signaling cascade. Mesothelin (encoded by *MSL*) was less expressed in lumA BC harboring high levels of LINC01087. *MSLN* has been described to promote invasion and metastasis in breast cancer cells [76]. Similarly, the overexpression of *MSL* in TNBC has been correlated with basal-like phenotype, as well as distant metastases and decreased survival [42]. The mechanism behind the metastatic potential of *MSL* overexpression has been attributed to its ability to stimulate the expression of matrix metalloproteinases (MMPs) -7 and -9 which play a major role in tumor progression and metastasis, for instance in pancreatic and ovarian cancers [77,78].

Based on the previous observations, we could speculate that the deregulation of LINC01087 has an impact on BC invasiveness and metastasis. In luminal BCs, the overexpression of LINC01087 may be responsible for the downregulation of the pro-invasive and pro-metastatic *MSL* and S100 proteins. By contrast, the downregulation of LINC01087 in TNBC would promote the synthesis of these factors thus increasing tumor aggressiveness, and reduce patient survival. Further functional investigations will be necessary to confirm this hypothesis.

Carboxypeptidase A4 (CPA4) is an exo-carboxypeptidase whose overexpression has been linked with cancer progression in several types of malignancies. For instance, its accumulation is associated with aggressiveness and unfavorable prognosis in TNBC [41]. In lumB BC samples, *CPA4* was downregulated upon overexpression of LINC01087. Neurofilaments like NEFM (neurofilament medium polypeptide) show a deregulated expression in several malignancies. A frequent and cancer-specific DNA methylation-associated silencing of *NEFM* has been reported in BC and correlates with disease progression [36]. In TNBC, we witnessed a strong upregulation of *NEFM* in samples with a high level of LINC01087.

As a last example, *ABCC8* belongs to the ATP-binding cassette (ABC) transporter gene family that controls the exchange of various molecules across membranes, including drugs [79]. The contribution of ABC genes in cancer progression and chemo-resistance, as well as their role in the prediction of therapy outcome and prognosis, is established [80,81]. Surprisingly, in BC patients, low levels of *ABCC8* have been associated with poor prognostic and predictive clinical markers (i.e. high expression of the proliferation marker Ki67, ER-negative status, or high grade tumors) [82,83]. Accordingly, the expression of *ABCC8* was increased in TNBC harboring enhanced level of LINC01087.

Collectively, by confronting our *in silico* data with the literature, multiple variations of genes observed upon increased expression of LINC01087 in TNBC and luminal BC subtypes support a tumor suppressive activity of this lncRNA. However, further wet-lab experiments will be needed to validate the molecular targets/interactors of LINC01087 in BC. Such basic knowledge could ultimately be exploited for therapeutic purposes.

## 6. Conclusions

In summary, LINC01087 is an intergenic lncRNA involved in breast carcinogenesis. Detection of LINC01087 downregulation represents a potential biomarker for the diagnosis and prognosis of TNBC patients, while its upregulation could be exploited for the diagnosis and prognosis of luminal BC patients. Such diagnostic and prognostic indicators may contribute to improve treatment management of BCs.

## Authors' Contributions

F.D.E.D.P. and V.D.M. performed most of the experiments. V.D. contributed to the transcriptomic experiment. M.K. and G.S. performed most of the bioinformatics and statistical analyses. V.D.M., M.K., B.U.R., C.C.K., A.V. and R.G. elaborated and interpreted the RNA-sequencing data. A.B. and D.M. performed the cryosection of tissue samples and contributed in laser-microdissection. G.B. and M.D. enrolled and selected patients in the clinical areas, and collected biological materials.

F.D.E.D.P., J.G.P. and M.C.M. prepared the figures. F.D.E.D.P., J.G.P., G. K., M.C.M and F.S. conceived the study, interpreted the data, supervised the whole set of the experiments, wrote and revised the manuscript. All authors have contributed, read and agreed to the published version of the manuscript.

### Declaration of Competing Interest

F.D.E.D.P., V.D.M., J.G.P., G.K., M.C.M. and F.S. are listed as co-inventors on a deposited patent that is under consideration for acceptance. All the authors declare no conflict of interest.

### Fundings

This research did not receive any specific grant from funding agencies in the public, commercial, or not-for-profit sectors.

### Availability of Data and Materials

The datasets used in the current study for *in silico* analyses were published previously as indicated in **Supplementary Table S16**.

RNA-seq data and clinical data of BC patients from the TCGA program were downloaded from the website Genomic Data Commons (<https://portal.gdc.cancer.gov>). Breast cell lines data were downloaded from the Expression Atlas database (<http://www.ebi.ac.uk/gxa>). Data for determining the mutational status of the BC samples have been downloaded from cBioPortal (<https://www.cbioportal.org>). Survival curves and forest plots were plotted using the online survival analysis tool “Kaplan-Meier Plotter” (<http://kmpplot.com/analysis/>), and the individual datasets used for the estimation of each survival curve are listed in **Supplementary Table S3**. GO terms annotations were performed using the Ensembl BioMart tool ([www.ensembl.org](http://www.ensembl.org)). KEGG and REACTOME pathways annotations were performed by means of the Comparative Toxicogenomics Database (ctdbase.org). GO, KEGG and REACTOME enrichment analyses were performed with g:GOST tool, from g:Profiler (<http://bit.cs.ut.ee/gprofiler/>). PPI network was computed using the application programming interface (API) of the STRING database ([string-db.org](http://string-db.org)).

### Acknowledgements

J.G.P. is supported by the Seerave Foundation, the Association Française d’Hépatologie (AFEF) and the SIRIC Cancer Research and Personalized Medicine (CARPEM). B.U.R. is supported by the National Science Center PL grant (2018/31/B/NZ2/01940). F.S. is supported by Regional/MIUR funds (Satin, Ciro, Campania Bioscience and Oncology 2020 (DGR n.7-15/01/2020) Projects) to fight against the oncological group of diseases. G.K. is supported by the Ligue contre le Cancer (équipe labellisée); Agence Nationale de la Recherche (ANR)–Projets blancs; ANR under the frame of E-Rare-2, the ERA-Net for Research on Rare Diseases; Association pour la recherche sur le cancer (ARC); Cancéropôle Ile-de-France; Chancellerie des universités de Paris (Legs Poix); Fondation pour la Recherche Médicale (FRM); a donation by Elior; European Research Area Network on Cardiovascular Diseases (ERA-CVD, MINOTAUR); Gustave Roussy Odyssey, the European Union Horizon 2020 Project Oncobiome; Fondation Carrefour; High-end Foreign Expert Program in China (GDW20171100085), Institut National du Cancer (INCa); Inserm (HTE); Institut Universitaire de France; LeDucq Foundation; the LabEx Immuno-Oncology; the RHU Torino Lumière; the Seerave Foundation; the SIRIC Stratified Oncology Cell DNA Repair and Tumor Immune Elimination (SOCRATE); and the SIRIC Cancer Research and Personalized Medicine (CARPEM).

### Appendix A. Supplementary data

Supplementary material related to this article can be found, in the

online version, at doi:<https://doi.org/10.1016/j.phrs.2020.105249>.

### References

- [1] N. Harbeck, F. Penault-Llorca, J. Cortes, M. Gnant, N. Houssami, P. Poortmans, K. Ruddy, J. Tsang, F. Cardoso, Breast cancer, Nat. Rev. Dis. Primer. 5 (2019) 1–31, <https://doi.org/10.1038/s41572-019-0111-2>.
- [2] E.A. Rakha, A.R. Green, Molecular classification of breast cancer: what the pathologist needs to know, Pathology (Phila.) 49 (2017) 111–119, <https://doi.org/10.1016/j.pathol.2016.10.012>.
- [3] A.G. Waks, E.P. Winer, Breast Cancer Treatment: A Review, JAMA. 321 (2019) 288–300, <https://doi.org/10.1001/jama.2018.19323>.
- [4] P. Schmid, S. Adams, H.S. Rugo, A. Schneeweiss, C.H. Barrios, H. Iwata, V. Diéras, R. Hegg, S.-A. Im, G.S. Wright, V. Henschel, L. Molinero, S.Y. Chui, R. Funke, A. Husain, E.P. Winer, S. Loi, L.A. Emens, Atezolizumab and Nab-Paclitaxel in Advanced Triple-Negative Breast Cancer, N. Engl. J. Med. (2018), <https://doi.org/10.1056/NEJMoa1809615>.
- [5] M. Robson, S.-A. Im, E. Senkus, B. Xu, S.M. Domchek, N. Masuda, S. Delalage, W. Li, N. Tung, A. Armstrong, W. Wu, C. Goessl, S. Runswick, P. Conte, Olaparib for Metastatic Breast Cancer in Patients with a Germline BRCA Mutation, N. Engl. J. Med. 377 (2017) 523–533, <https://doi.org/10.1056/NEJMoa1706450>.
- [6] F. Pareja, J.S. Reis-Filho, Triple-negative breast cancers - a panoply of cancer types, Nat. Rev. Clin. Oncol. 15 (2018) 347–348, <https://doi.org/10.1038/s41571-018-0001-7>.
- [7] M. Royce, T. Bachelot, C. Villanueva, M. Özgüroglu, S.J. Azevedo, F.M. Cruz, M. Debled, R. Hegg, T. Toyama, C. Falkson, J. Jeong, V. Srimuninnimit, W. J. Gradishar, C. Arce, A. Ridolfi, C. Lin, F. Cardoso, Everolimus Plus Endocrine Therapy for Postmenopausal Women With Estrogen Receptor-Positive, Human Epidermal Growth Factor Receptor 2-Negative Advanced Breast Cancer: A Clinical Trial, JAMA Oncol. 4 (2018) 977–984, <https://doi.org/10.1001/jamaoncol.2018.0060>.
- [8] G.N. Hortobagyi, S.M. Stemmer, H.A. Burris, Y.-S. Yap, G.S. Sonke, S. Paluch-Shimon, M. Campone, K.L. Blackwell, F. André, E.P. Winer, W. Janni, S. Verma, P. Conte, C.L. Arteaga, D.A. Cameron, K. Petrakova, L.L. Hart, C. Villanueva, A. Chan, E. Jakobsen, A. Nusch, O. Burdaeva, E.-M. Grischke, E. Alba, E. Wist, N. Marschner, A.M. Favret, D. Yardley, T. Bachelot, L.-M. Tseng, S. Blau, F. Xuan, F. Souami, M. Miller, C. Germa, S. Hirawat, J. O’Shaughnessy, Ribociclib as First-Line Therapy for HR-Positive, Advanced Breast Cancer, N. Engl. J. Med. 375 (2016) 1738–1748, <https://doi.org/10.1056/NEJMoa1609709>.
- [9] M.J. Duffy, N. Harbeck, M. Nap, R. Molina, A. Nicolini, E. Senkus, F. Cardoso, Clinical use of biomarkers in breast cancer: Updated guidelines from the European Group on Tumor Markers (EGTM), Eur. J. Cancer. 75 (2017) 284–298, <https://doi.org/10.1016/j.ejca.2017.01.017>.
- [10] B.Z. Clark, A. Onisko, B. Assylbekova, X. Li, R. Bhargava, D.J. Dabbs, Breast cancer global tumor biomarkers: a quality assurance study of intratumoral heterogeneity, Mod. Pathol. Off. J. U. S. Can. Acad. Pathol. Inc. 32 (2019) 354–366, <https://doi.org/10.1038/s41379-018-0153-0>.
- [11] T. Tian, M. Wang, S. Lin, Y. Guo, Z. Dai, K. Liu, P. Yang, C. Dai, Y. Zhu, Y. Zheng, P. Xu, W. Zhu, Z. Dai, The Impact of lncRNA Dysregulation on Clinicopathology and Survival of Breast Cancer: A Systematic Review and Meta-analysis, Mol. Ther. - Nucleic Acids. 12 (2018) 359–369, <https://doi.org/10.1016/j.omtn.2018.05.018>.
- [12] S. Di Cecilia, F. Zhang, A. Sancho, S.D. Li, F. Aguilo, Y. Sun, M. Rengasamy, W. Zhang, L.D. Vecchio, F. Salvatore, M.J. Walsh, RBM5-AS1 is critical for self-renewal of colon cancer stem-like cells, Cancer Res. 76 (2016) 5615–5627, <https://doi.org/10.1158/0008-5472.CAN-15-1824>.
- [13] Y. Chi, D. Wang, J. Wang, W. Yu, J. Yang, Long Non-Coding RNA in the Pathogenesis of Cancers, Cells. 8 (2019), <https://doi.org/10.3390/cells8091015>.
- [14] B. Bánfai, H. Jia, J. Khatun, E. Wood, B. Risk, W.E. Gundling, A. Kundaje, H. P. Gunawardena, Y. Yu, L. Xie, K. Krajewski, B.D. Strahl, X. Chen, P. Bickel, M. C. Giddings, J.B. Brown, L. Lipovich, Long noncoding RNAs are rarely translated in two human cell lines, Genome Res. 22 (2012) 1646–1657, <https://doi.org/10.1101/gr.134767.111>.
- [15] J. Harrow, A. Frankish, J.M. Gonzalez, E. Tapanari, M. Diekhans, F. Kokocinski, B. L. Aken, D. Barrell, A. Zadissa, S. Searle, I. Barnes, A. Bignell, V. Boychenko, T. Hunt, M. Kay, G. Mukherjee, J. Rajan, G. Despacio-Reyes, G. Saunders, C. Steward, R. Harte, M. Lin, C. Howald, A. Tanzer, T. Derrien, J. Chrast, N. Walters, S. Balasubramanian, B. Pei, M. Tress, J.M. Rodriguez, I. Ezkurdia, J. van Baren, M. Brent, D. Haussler, M. Kellis, A. Valencia, A. Reymond, M. Gerstein, R. Guigó, T.J. Hubbard, GENCODE: the reference human genome annotation for The ENCODE Project, Genome Res. 22 (2012) 1760–1774, <https://doi.org/10.1101/gr.135350.111>.
- [16] J.K. Dhanoa, R.S. Sethi, R. Verma, J.S. Arora, C.S. Mukhopadhyay, Long non-coding RNA: its evolutionary relics and biological implications in mammals: a review, J. Anim. Sci. Technol. 60 (2018), <https://doi.org/10.1186/s40781-018-0183-7>.
- [17] X.C. Quek, D.W. Thomson, J.L.V. Maag, N. Bartonicek, B. Signal, M.B. Clark, B. S. Gloss, M.E. Dinger, lncRNADB v2.0: expanding the reference database for functional long noncoding RNAs, Nucleic Acids Res. 43 (2015) D168–173, <https://doi.org/10.1093/nar/gku988>.
- [18] C.P. Ponting, P.L. Oliver, W. Reik, Evolution and Functions of Long Noncoding RNAs, Cell. 136 (2009) 629–641, <https://doi.org/10.1016/j.cell.2009.02.006>.
- [19] C. Mathias, E.P. Zambalde, P. Rask, D.F. Gradia, J.C. de Oliveira, Long non-coding RNAs differential expression in breast cancer subtypes: What do we know? Clin. Genet 95 (2019) 558–568, <https://doi.org/10.1111/cge.13502>.



- [20] W.-X. Peng, J.-G. Huang, L. Yang, A.-H. Gong, Y.-Y. Mo, Linc-RoR promotes MAPK/ERK signaling and confers estrogen-independent growth of breast cancer, *Mol. Cancer* 16 (2017) 161, <https://doi.org/10.1186/s12943-017-0727-3>.
- [21] Y.-M. Chen, Y. Liu, H.-Y. Wei, K.-Z. Lv, P. Fu, Linc-ROR induces epithelial-mesenchymal transition and contributes to drug resistance and invasion of breast cancer cells, *Tumour Biol. J. Int. Soc. Oncodevelopmental Biol. Med.* 37 (2016) 10861–10870, <https://doi.org/10.1007/s13277-016-4909-1>.
- [22] Q.-Y. Huang, G.-F. Liu, X.-L. Qian, L.-B. Tang, Q.-Y. Huang, L.-X. Xiong, Long Non-Coding RNA: Dual Effects on Breast Cancer Metastasis and Clinical Applications, *Cancers* 11 (2019), <https://doi.org/10.3390/cancers11111802>.
- [23] A. Dobin, C.A. Davis, F. Schlesinger, J. Drenkow, C. Zaleski, S. Jha, P. Batut, M. Chaisson, T.R. Gingeras, STAR: ultrafast universal RNA-seq aligner, *Bioinforma. Oxf. Engl.* 29 (2013) 15–21, <https://doi.org/10.1093/bioinformatics/bts635>.
- [24] An Integrated Encyclopedia of DNA Elements in the Human Genome, *Nature* 489 (2012) 57–74, <https://doi.org/10.1038/nature11247>.
- [25] B. Li, C.N. Dewey, RSEM: accurate transcript quantification from RNA-Seq data with or without a reference genome, *BMC Bioinformatics.* 12 (2011) 323, <https://doi.org/10.1186/1471-2105-12-323>.
- [26] X. Robin, N. Turck, A. Hainard, N. Tiberti, F. Lisacek, J.-C. Sanchez, M. Müller, pROC: an open-source package for R and S+ to analyze and compare ROC curves, *BMC Bioinformatics.* 12 (2011) 77, <https://doi.org/10.1186/1471-2105-12-77>.
- [27] A. Bunn, M. Korpela, An introduction to dprR, *(n.d.)* 16.
- [28] D. Szklarczyk, J.H. Morris, H. Cook, M. Kuhn, S. Wyder, M. Simonovic, A. Santos, N.T. Doncheva, A. Roth, P. Bork, L.J. Jensen, C. von Mering, The STRING database in 2017: quality-controlled protein–protein association networks, made broadly accessible, *Nucleic Acids Res.* 45 (2017) D362–D368, <https://doi.org/10.1093/nar/gkw937>.
- [29] Á. Nagy, A. Lánckzy, O. Menyárt, B. Gyórfy, Validation of miRNA prognostic power in hepatocellular carcinoma using expression data of independent datasets, *Sci. Rep.* 8 (2018) 1–9, <https://doi.org/10.1038/s41598-018-27521-y>.
- [30] E.A. Rakha, I.O. Ellis, Triple-negative/basal-like breast cancer: review, *Pathology (Phila.)* 41 (2009) 40–47, <https://doi.org/10.1080/00313020802563510>.
- [31] E.S. McDonald, A.S. Clark, J. Tchou, P. Zhang, G.M. Freedman, Clinical Diagnosis and Management of Breast Cancer, *J. Nucl. Med. Off. Publ. Soc. Nucl. Med.* 57 (Suppl 1) (2016) 9S–16S, <https://doi.org/10.2967/jnumed.115.157834>.
- [32] N.M. Tung, J.E. Garber, BRCA 1/2 testing: therapeutic implications for breast cancer management, *Br. J. Cancer.* 119 (2018) 141–152, <https://doi.org/10.1038/s41416-018-0127-5>.
- [33] J. Huszno, E. Grzybowska, TP53 mutations and SNPs as prognostic and predictive factors in patients with breast cancer, *Oncol. Lett.* 16 (2018) 34–40, <https://doi.org/10.3892/ol.2018.8627>.
- [34] E. Buache, N. Etique, F. Alpy, I. Stoll, M. Muckensturm, B. Reina-San-Martin, M. P. Chenard, C. Tomasetto, M.C. Rio, Deficiency in trefoil factor 1 (TFF1) increases tumorigenicity of human breast cancer cells and mammary tumor development in TFF1-knockout mice, *Oncogene* 30 (2011) 3261–3273, <https://doi.org/10.1038/onc.2011.41>.
- [35] X. Chen, J.M. Corbin, G.J. Tipton, L.V. Yang, A.S. Asch, M.J. Ruiz-Echevarria, THE TMEFF2 TUMOR SUPPRESSOR MODULATES INTEGRIN EXPRESSION, RHOA ACTIVATION AND MIGRATION OF PROSTATE CANCER CELLS, *Biochim. Biophys. Acta.* 1843 (2014) 1216–1224, <https://doi.org/10.1016/j.bbamac.2014.03.005>.
- [36] M.F. Calmon, J. Jeschke, W. Zhang, M. Dhir, C. Siebenkäs, A. Herrera, H.-C. Tsai, H.M. O'Hagan, E.P. Pappou, C.M. Hooker, T. Fu, K.E. Schuebel, E. Gabrielson, P. Rahal, J.G. Herman, S.B. Baylin, N. Ahuja, Epigenetic silencing of neurofilament genes promotes an aggressive phenotype in breast cancer, *Epigenetics* 10 (2015) 622–632, <https://doi.org/10.1080/15592294.2015.1050173>.
- [37] A. Sharma, M. Albahrani, W. Zhang, C.N. Kufel, S.R. James, K. Odunsi, D. Klinkbeil, A.R. Karpf, Epigenetic activation of POTE genes in ovarian cancer, *Epigenetics* 14 (2019) 185–197, <https://doi.org/10.1080/15592294.2019.1581590>.
- [38] Evolutionary Dynamics of the POTE Gene Family in Human and Nonhuman Primates, *(n.d.)*. <https://www.ncbi.nlm.nih.gov/pmc/articles/PMC7073761/> (accessed May 30, 2020).
- [39] A.R. Bresnick, D.J. Weber, D.B. Zimmer, S100 proteins in cancer, *Nat. Rev. Cancer.* 15 (2015) 96–109, <https://doi.org/10.1038/nrc3893>.
- [40] K.M. Coyle, J.P. Murphy, D. Vidovic, A. Vaghar-Kashani, C.A. Dean, M. Sultan, D. Clements, M. Wallace, M.L. Thomas, A. Hundert, C.A. Giacomantonio, L. Helyer, S.A. Gujar, P.W.K. Lee, I.C.G. Weaver, P. Marcato, Breast cancer subtype dictates DNA methylation and ALDH1A3-mediated expression of tumor suppressor RARRES1, *Oncotarget* 7 (2016) 44096–44112, <https://doi.org/10.18632/oncotarget.9858>.
- [41] T. Handa, A. Katayama, T. Yokobori, A. Yamane, T. Fujii, S. Obayashi, S. Kurozumi, R. Kawabata-Iwakawa, N. Gombodorj, M. Nishiyama, T. Asao, K. Shirabe, H. Kuwano, T. Oyama, Carboxypeptidase A4 accumulation is associated with an aggressive phenotype and poor prognosis in triple-negative breast cancer, *Int. J. Oncol.* 54 (2019) 833–844, <https://doi.org/10.3892/ijo.2019.4675>.
- [42] G. Tozbykian, E. Brogi, K. Kadota, J. Catalano, M. Akram, S. Patil, A.Y. Ho, J. S. Reis-Filho, B. Weigelt, L. Norton, P.S. Adusumilli, H.Y. Wen, Mesothelin Expression in Triple Negative Breast Carcinomas Correlates Significantly with Basal-Like Phenotype, Distant Metastases and Decreased Survival, *PLoS ONE* 9 (2014), <https://doi.org/10.1371/journal.pone.0114900>.
- [43] J. Del Bano, R. Florès-Florés, E. Josselin, A. Goubard, L. Ganier, R. Castellano, P. Chames, D. Baty, B. Kerfelec, A Bispecific Antibody-Based Approach for Targeting Mesothelin in Triple Negative Breast Cancer, *Front. Immunol.* 10 (2019), <https://doi.org/10.3389/fimmu.2019.01593>.
- [44] H. Liu, Y. Kato, S.A. Erzinger, G.M. Kiriakova, Y. Qian, D. Palmieri, P.S. Steeg, J. E. Price, The role of MMP-1 in breast cancer growth and metastasis to the brain in a xenograft model, *BMC Cancer* 12 (2012) 583, <https://doi.org/10.1186/1471-2407-12-583>.
- [45] Q.-M. Wang, L. Lv, Y. Tang, L. Zhang, L.-F. Wang, MMP-1 is overexpressed in triple-negative breast cancer tissues and the knockdown of MMP-1 expression inhibits tumor cell malignant behaviors in vitro, *Oncol. Lett.* 17 (2019) 1732–1740, <https://doi.org/10.3892/ol.2018.9779>.
- [46] M.W. Nasser, Z. Qamri, Y.S. Deol, J. Ravi, C.A. Powell, P. Trikha, R. A. Schwendener, X.-F. Bai, K. Shilo, X. Zou, G. Leone, R. Wolf, S.H. Yuspa, R. K. Ganju, S100A7 enhances mammary tumorigenesis through upregulation of inflammatory pathways, *Cancer Res.* 72 (2012) 604–615, <https://doi.org/10.1158/0008-5472.CAN-11-0669>.
- [47] Y. Liu, Y. Cai, L. Liu, Y. Wu, X. Xiong, Crucial biological functions of CCL7 in cancer, *PeerJ* 6 (2018), <https://doi.org/10.7717/peerj.4928>.
- [48] microRNA-130a suppresses breast cancer cell migration and invasion by targeting FOSL1 and upregulating ZO-1 - Chen - 2018, *Journal of Cellular Biochemistry - Wiley Online Library*, *(n.d.)*. <https://onlinelibrary.wiley.com/doi/abs/10.1002/jcb.26739> (accessed May 30, 2020).
- [49] Enhancer transcription reveals subtype-specific gene expression programs controlling breast cancer pathogenesis, *(n.d.)*. <https://www.ncbi.nlm.nih.gov/pmc/articles/PMC5793780/> (accessed May 30, 2020).
- [50] A. Singh, J.J. Nunes, B. Ateeq, Role and therapeutic potential of G-protein coupled receptors in breast cancer progression and metastases, *Eur. J. Pharmacol.* 763 (2015) 178–183, <https://doi.org/10.1016/j.ejphar.2015.05.011>.
- [51] GPCR Modulation in Breast Cancer, *(n.d.)*. <https://www.ncbi.nlm.nih.gov/pmc/articles/PMC6321247/> (accessed May 22, 2020).
- [52] K.L. Eales, K.E.R. Hollinshead, D.A. Tennant, Hypoxia and metabolic adaptation of cancer cells, *Oncogenesis* 5 (2016), <https://doi.org/10.1038/ocncis.2015.50> e190–e190.
- [53] Erythropoietin drives breast cancer progression by activation of its receptor EPOR | Oncotarget, *(n.d.)*. <https://www.oncotarget.com/article/16368/text/> (accessed May 30, 2020).
- [54] Y. Li, C. Tu, H. Wang, D.N. Silverman, S.C. Frost, Catalysis and pH Control by Membrane-associated Carbonic Anhydrase IX in MDA-MB-231 Breast Cancer Cells, *J. Biol. Chem.* 286 (2011) 15789–15796, <https://doi.org/10.1074/jbc.M110.188524>.
- [55] A. Güttler, K. Theuerkorn, A. Riemann, H. Wichmann, J. Kessler, O. Thews, M. Bache, D. Vordermark, Cellular and radiobiological effects of carbonic anhydrase IX in human breast cancer cells, *Oncol. Rep.* 41 (2019) 2585–2594, <https://doi.org/10.3892/or.2019.7001>.
- [56] S.C. Chafe, P.C. McDonald, S. Saberi, O. Nemirovsky, G. Venkateswaran, S. Burugu, D. Gao, A. Delaidelli, A.H. Kyle, J.H.E. Baker, J.A. Gillespie, A. Bashashati, A. I. Minchinton, Y. Zhou, S.P. Shah, S. Dedhar, Targeting Hypoxia-Induced Carbonic Anhydrase IX Enhances Immune-Checkpoint Blockade Locally and Systemically, *Cancer Immunol. Res.* 7 (2019) 1064–1078, <https://doi.org/10.1158/2326-6066.CIR-18-0657>.
- [57] L.D. Naorem, V.S. Prakash, M. Muthaiyan, A. Venkatesan, Comprehensive analysis of dysregulated lncRNAs and their competing endogenous RNA network in triple-negative breast cancer, *Int. J. Biol. Macromol.* 145 (2020) 429–436, <https://doi.org/10.1016/j.ijbiomac.2019.12.196>.
- [58] R. Tripathi, I. Aier, P. Chakraborty, P.K. Varadwaj, Unravelling the role of long non-coding RNA - LINC01087 in breast cancer, *Non-Coding RNA Res.* 5 (2020) 1–10, <https://doi.org/10.1016/j.ncrna.2019.12.002>.
- [59] F. Pareja, J.S. Reis-Filho, Triple-negative breast cancers — a panoply of cancer types, *Nat. Rev. Clin. Oncol.* (2018), <https://doi.org/10.1038/s41571-018-0001-7>.
- [60] P. Bertheau, J. Lehmann-Che, M. Varna, A. Dumay, B. Poirrot, R. Porcher, E. Turpin, L.-F. Plassa, A. de Roquancourt, E. Bourstyn, P. de Cremoux, A. Janin, S. Giacchetti, M. Espié, H. de Thé, p53 in breast cancer subtypes and new insights into response to chemotherapy, *The Breast* 22 (2013) S27–S29, <https://doi.org/10.1016/j.breast.2013.07.005>.
- [61] M.S. Greenblatt, P.O. Chappuis, J.P. Bond, N. Hamel, W.D. Foulkes, TP53 Mutations in Breast Cancer Associated with BRCA1 or BRCA2 Germ-line Mutations: Distinctive Spectrum and Structural Distribution, *Cancer Res.* 61 (2001) 4092–4097 (accessed August 9, 2019), <https://cancerres.aacrjournals.org/content/61/10/4092>.
- [62] U.M. Zanger, M. Schwab, Cytochrome P450 enzymes in drug metabolism: regulation of gene expression, enzyme activities, and impact of genetic variation, *Pharmacol. Ther.* 138 (2013) 103–141, <https://doi.org/10.1016/j.pharmthera.2012.12.007>.
- [63] K. Purnapatre, S.K. Khattar, K.S. Saini, Cytochrome P450s in the development of target-based anticancer drugs, *Cancer Lett.* 259 (2008) 1–15, <https://doi.org/10.1016/j.canlet.2007.10.024>.
- [64] C. Bergenfelz, A. Gaber, R. Allaoui, M. Mehmeti, K. Jirstrom, T. Leandersson, K. Leandersson, S100A9 expressed in ER(-)PgR(-) breast cancers induces inflammatory cytokines and is associated with an impaired overall survival, *Br. J. Cancer.* 113 (2015) 1234–1243, <https://doi.org/10.1038/bjc.2015.346>.
- [65] G. Kroemer, L. Senovilla, L. Galluzzi, F. André, L. Zitvogel, Natural and therapy-induced immunosurveillance in breast cancer, *Nat. Med.* 21 (2015) 1128–1138, <https://doi.org/10.1038/nm.3944>.
- [66] F.R. Greten, S.I. Grivnenkov, Inflammation and Cancer: Triggers, Mechanisms, and Consequences, *Immunity* 51 (2019) 27–41, <https://doi.org/10.1016/j.immuni.2019.06.025>.
- [67] K. Taniguchi, M. Karin, NF-κB, inflammation, immunity and cancer: coming of age, *Nat. Rev. Immunol.* 18 (2018) 309–324, <https://doi.org/10.1038/nri.2017.142>.
- [68] V. Sladky, F. Schuler, L.L. Fava, A. Villunger, The resurrection of the PIDDosome – emerging roles in the DNA-damage response and centrosome surveillance, *J. Cell Sci.* 130 (2017) 3779–3787, <https://doi.org/10.1242/jcs.203448>.

- [69] Y. Lin, W. Ma, S. Benchimol, Pidd, a new death-domain-containing protein, is induced by p53 and promotes apoptosis, *Nat. Genet* 26 (2000) 122–127, <https://doi.org/10.1038/79102>.
- [70] J. Yi, L. Ren, D. Li, J. Wu, W. Li, G. Du, J. Wang, Trefoil factor 1 (TFF1) is a potential prognostic biomarker with functional significance in breast cancers, *Biomed. Pharmacother.* 124 (2020) 109827, <https://doi.org/10.1016/j.biopha.2020.109827>.
- [71] J.-M. Sun, V.A. Spencer, L. Li, H. Yu Chen, J. Yu, J.R. Davie, Estrogen regulation of trefoil factor 1 expression by estrogen receptor  $\alpha$  and Sp proteins, *Exp. Cell Res.* 302 (2005) 96–107, <https://doi.org/10.1016/j.yexcr.2004.08.015>.
- [72] M. Soutto, Z. Chen, M.A. Saleh, A. Katsha, S. Zhu, A. Zaika, A. Belkhir, W. El-Rifai, TFF1 activates p53 through down-regulation of miR-504 in gastric cancer, *Oncotarget* 5 (2014) 5663–5673, <https://doi.org/10.18632/oncotarget.2156>.
- [73] M. Busch, J. Große-Kreul, J.J. Wirtz, M. Beier, H. Stephan, B. Royer-Pokora, K. Metz, N. Dünker, Reduction of the tumorigenic potential of human retinoblastoma cell lines by TFF1 overexpression involves p53/caspase signaling and miR-18a regulation, *Int. J. Cancer* 141 (2017) 549–560, <https://doi.org/10.1002/ijc.30768>.
- [74] K. A. K. Vl, Dramatic dysbalancing of the Wnt pathway in breast cancers, *Sci. Rep.* 8 (2018), <https://doi.org/10.1038/s41598-018-25672-6>, 7329–7329.
- [75] S.-G. Pohl, N. Brook, M. Agostino, F. Arfuso, A.P. Kumar, A. Dharmarajan, Wnt signaling in triple-negative breast cancer, *Oncogenesis* 6 (2017) e310, <https://doi.org/10.1038/oncsis.2017.14>.
- [76] Y. Wang, L. Wang, D. Li, H.B. Wang, Q.F. Chen, Mesothelin promotes invasion and metastasis in breast cancer cells, *J. Int. Med. Res.* 40 (2012) 2109–2116, <https://doi.org/10.1177/030006051204000608>.
- [77] S.-H. Chen, W.-C. Hung, P. Wang, C. Paul, K. Konstantopoulos, Mesothelin Binding to CA125/MUC16 Promotes Pancreatic Cancer Cell Motility and Invasion via MMP-7 Activation, *Sci. Rep.* 3 (2013) 1870, <https://doi.org/10.1038/srep01870>.
- [78] M.-C. Chang, C.-A. Chen, P.-J. Chen, Y.-C. Chiang, Y.-L. Chen, T.-L. Mao, H.-W. Lin, W.-H. Lin Chiang, W.-F. Cheng, Mesothelin enhances invasion of ovarian cancer by inducing MMP-7 through MAPK/ERK and JNK pathways, *Biochem. J.* 442 (2012) 293–302, <https://doi.org/10.1042/BJ20110282>.
- [79] H. Glavinas, P. Krajcsi, J. Cserepes, B. Sarkadi, The role of ABC transporters in drug resistance, metabolism and toxicity, *Curr. Drug Deliv.* 1 (2004) 27–42, <https://doi.org/10.2174/1567201043480036>.
- [80] J.I. Fletcher, M. Haber, M.J. Henderson, M.D. Norris, ABC transporters in cancer: more than just drug efflux pumps, *Nat. Rev. Cancer* 10 (2010) 147–156, <https://doi.org/10.1038/nrc2789>.
- [81] M. Pasello, A.M. Giudice, K. Scotlandi, The ABC subfamily A transporters: Multifaceted players with incipient potentialities in cancer, *Semin. Cancer Biol.* (2019), <https://doi.org/10.1016/j.semcancer.2019.10.004>.
- [82] V. Hlaváč, V. Brynychová, R. Václavíková, M. Ehrlichová, D. Vrána, V. Pecha, R. Koževnikovová, M. Trnková, J. Gatěk, D. Kopperová, I. Gut, P. Souček, The expression profile of ATP-binding cassette transporter genes in breast carcinoma, *Pharmacogenomics* 14 (2013) 515–529, <https://doi.org/10.2217/pgs.13.26>.
- [83] P. Soucek, V. Hlavac, K. Elsnerova, R. Vaclavikova, R. Kozevnikovova, K. Raus, Whole exome sequencing analysis of ABC8 and ABCD2 genes associating with clinical course of breast carcinoma, *Physiol. Res.* 64 (Suppl 4) (2015) S549–557.